CHAPTER IV
RESULTS AND DISCUSSIONS

In this chapter, details will be separated into two parts. The first part contains the results and discussion from structure and morphology of as received MWNTs, modified MWNTs and synthesized composites. The second part focuses on the electrochemical measurements of modified electrodes using cyclic voltammetry, electrochemical impedance spectroscopy and galvanostatic charge-discharge. The results of these electrodes were compared and discussed.

4.1 Characterization of Functionalized MWNTs

4.1.1 Structural Characterization of Functionalized MWNTs

4.1.1.1 Surface Area and Pore Volume Characterization

Table 4.1 Structural parameters of as received MWNTs and MWNTs that were refluxed for 6, 12 and 18 hours

Sample	BET surface area (m^2/g)	Micropore area (m^2/g)	Micropore volume (cm^3/g)	Total pore volume (cm^3/g)
- As received MWNTs	346	313	0.12	0.13
- Refluxed MWNTs for 6 hours	432	408	0.17	0.17
- Refluxed MWNTs for 12 hours	528	512	0.22	0.23
- Refluxed MWNTs for 18 hours	571	556	0.27	0.28

The results of the nitrogen gas adsorption-desorption on as received MWNTs and functionalized MWNTs are listed in table 4.1. The BET specific surface area and the pore volume of as received MWNTs were 346 m^2/g and 0.13 cm^3/g, respectively. Whereas the specific surface area and the pore volume of the functionalized MWNTs increased with the increase of reflux time. Moreover, it was found that the specific surface area and the pore volume of MWNTs, which refluxed for 18 hours, were 571 m^2/g and 0.28 cm^3/g. Thus, this result could be concluded that the increasing specific surface area and pore volume of the modified MWNTs resulted from the chemical treatment time with concentrated of nitric acid.

4.1.1.2 Functionalization Characterization

The FTIR spectrums in the range of 1000 – 4000 cm^{-1} obtained from as received MWNTs and MWNTs, which were refluxed for 6, 12 and 18 hours, are showed in Figure 4.1. A board absorption band at 3,437 cm^{-1} was attributed to the hydroxyl group (υ OH). This band resulted from water and the -OH functional groups during the purification and functionalization process [28]. The peak at 1,776 cm^{-1} was concerned with the C=O stretching of carboxylic acid group (-COOH) and the peak at 1,630 cm^{-1} was associated with C=C stretching of the modified MWNTs [29,30]. The presence of –COOH groups on MWNTs surface increased the solubility of MWNTs in the solvents and the attachment of nanocrytalline metal oxides on the functionalized MWNTs with the covalent bond [31,32], as a result of acid treatment process, was confirmed by FTIR technique.

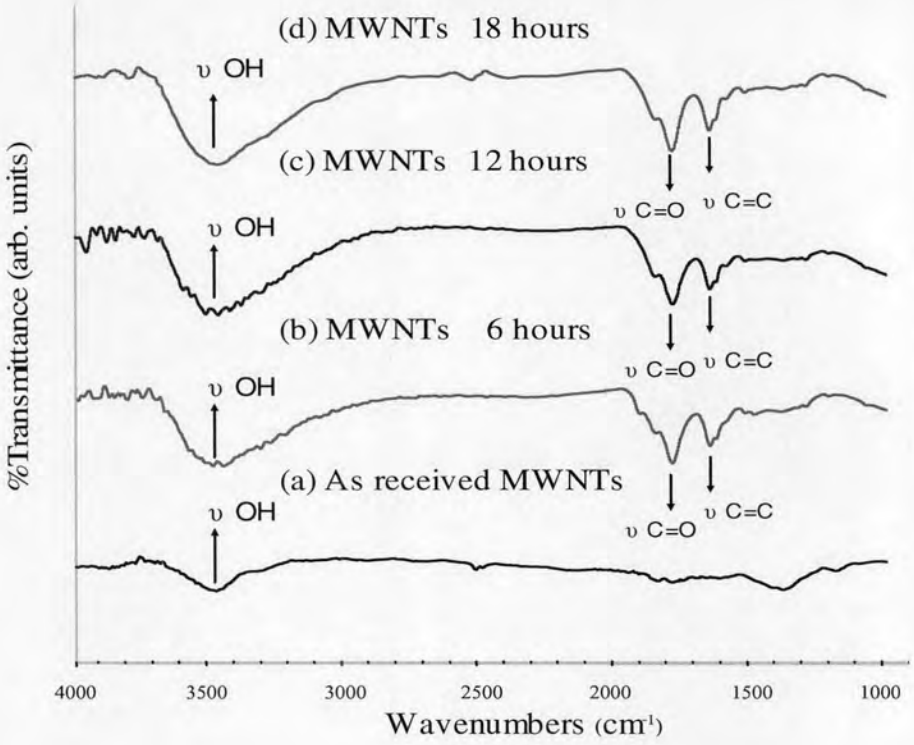

Figure 4.1 FTIR spectra of (a) as received MWNTs and (b, c and d) MWNTs that were refluxed for 6, 12 and 18 hours.

4.1.1.3 Crystallization Characterization

XRD analysis, which is the most useful technique for identification of crystalline structure, was employed to investigate the prepared samples. As showed in Figure 4.2 (a), the XRD pattern of as received MWNTs using nickel as catalyst during preparation process. MWNTs showed a typical peak of the (002) refraction at 2θ of MWNTs at 26.3^0 which was indexed to the reflection of hexagonal graphite [33]. Other small peaks corresponding to the catalytic impurities were also seen. The XRD patterns of the purified and functionalized MWNTs in Figure 4.2 (b-d) indicated that the metallic impurities of MWNTs were removed by acid treatment. Importantly, by applying the Scherrer equation on the intense peak of (002) reflection, the crystalline sizes of MWNTs were determined to be 9 nanometers.

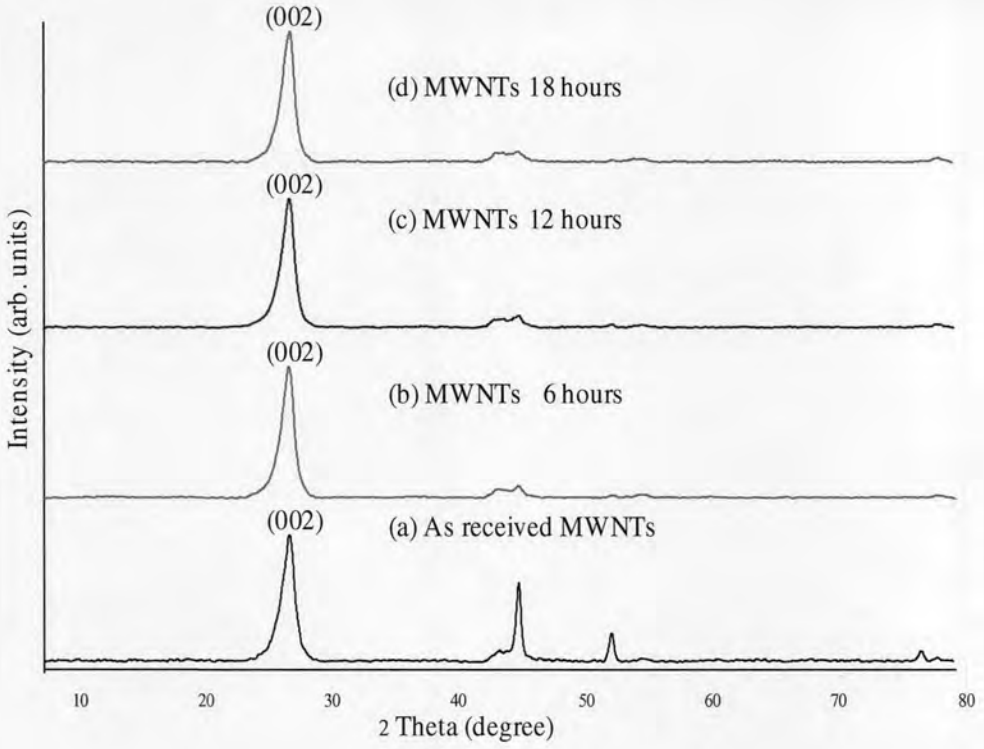

Figure 4.2 XRD patterns of (a) as received MWNTs and (b, c and d) MWNTs that were refluxed for 6, 12 and 18 hours.

4.1.2 Electrochemical Measurement of Functionalized MWNTs

The influence of reflux time on the electrochemical behavior, of the functionalized MWNTs is given in Figure 4.3. Carbon electrodes or EDLCs are normally well known that their capacitance obtained from charged surface of electrodes and electrolyte ions [34-40]. Normally, non faradaic process of EDLCs increases with increase in the reacted area of electrode. The charged storage capability is increased at the higher surface area due to the influence of carbon porosities. In Figure 4.3, the currents with increase in the time of reflux which the anodic current shifted positively while the cathodic current shifted negatively, and the specific capacitance of MWNTs, which refluxed for 6 hours, was significantly enhanced from 56.36 to 81.21 F/g for the refluxed MWNTs with 18 hours as showed in Figure 4.5. This result could be explained that the increasing specific capacitance of modified MWNTs resulted from the chemical treatment time which increased the specific surface area and the micropore volume of MWNTs.

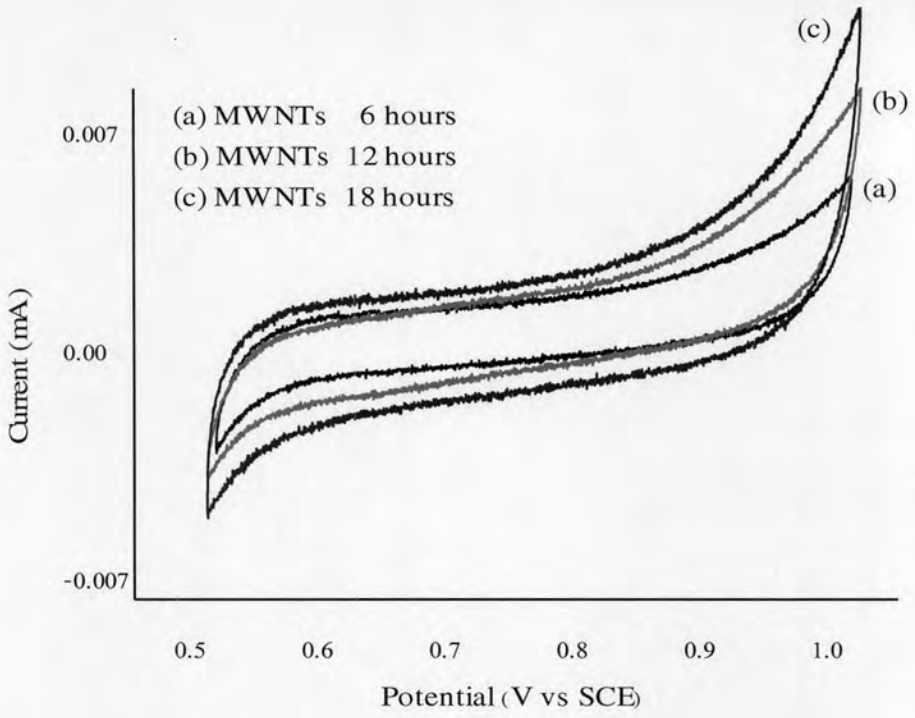

Figure 4.3 Cyclic voltammogram of (a, b and c) functionalized MWNTs that were refluxed for 6, 12 and 18 hours.

The comparison of complex plane plots for the functionalized MWNTs with varying times of reflux as illustrated in Figure 4.4. The diameter of semicircles at higher frequencies continued to decrease with the increase of reflux time. This clearly indicated that the resistance value was decreased with the increase in time of MWNTs reflux. In addition, the straight line in the lower frequency region was influenced by the diffusion of electrolyte ions to the porous electrodes [19-23]. In this case, the electrochemical capacitance and conductance of the refluxed MWNTs with 18 hours were the best among those of samples. This was caused by the changes in MWNTs structure, such as surface area and porosity during the chemical treatment.

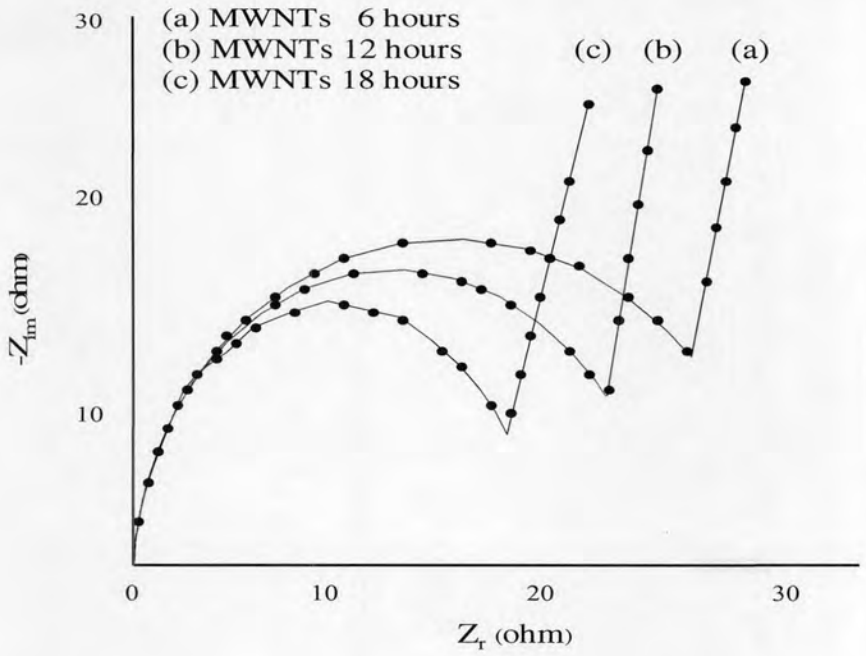

Figure 4.4 Complex-plane impedance spectra of (a, b and c) functionalized MWNTs that were refluxed for 6, 12 and 18 hours.

Figure 4.5 presents the symmetry of galvanostatic charge-discharge curves of MWNTs samples at an applied current of 10 mA. From this experiment, the symmetrical charge-discharge slope of MWNTs electrodes decreased, which exhibited the longer cycle life, with the increasing time of chemical treatment which could be calculated the capacitances by the equation 3.2 and found that the specific capacitance of the refluxed MWNTs with 18 hours was the highest of the other sample which in agreement with cyclic voltammetry and impedance spectroscopy observations. Furthermore, the effect of chemical treatment time on the average specific capacitance is given in Figure 4.6.

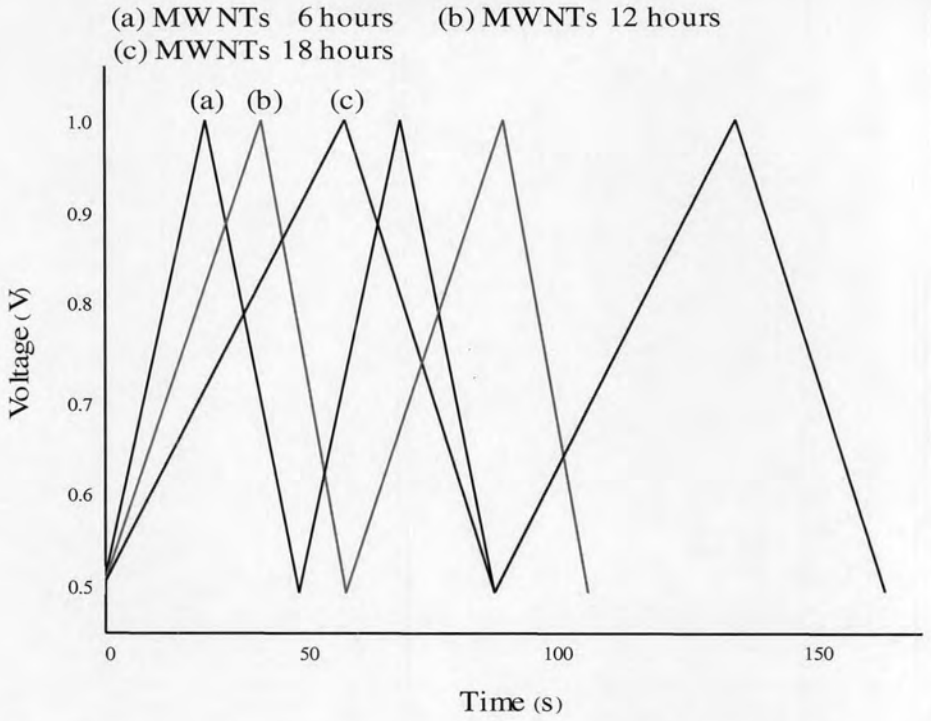

Figure 4.5 Galvanostatic charge-discharge of (a, b and c) functionalized MWNTs that were refluxed for 6, 12 and 18 hours.

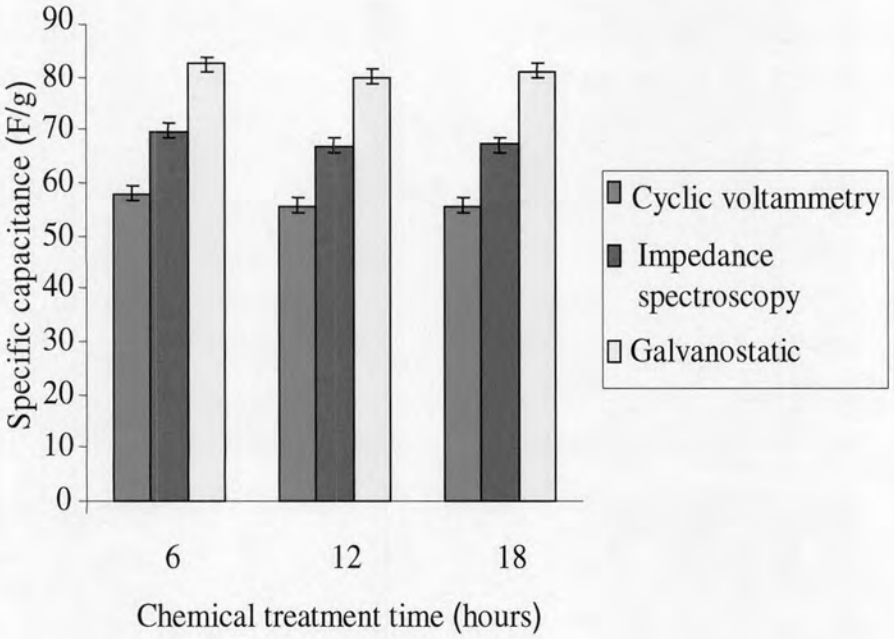

Figure 4.6 The effect of chemical treatment time on specific capacitance (F/g).

In this work, the refluxed MWNTs with 18 hours was brought to synthesize with the metal salts by chemical reduction to be the nanocrystalline composites for ECs.

4.2 Characterization of TiO_2/MWNTs Composites

4.2.1 Structural Characterization of TiO_2/MWNTs Composites

Figure 4.7 illustrates the XRD patterns of functionalized MWNTs and TiO_2/MWNTs composites with the various ratios. In Figure 4.7 (a), characteristic peak of MWNTs, which was located at 26.3^0, corresponded to the (002) refraction. TiO_2 in anatase phase was indexed from the patterns of TiO_2 composites in Figure 4.7 (b-f) at 25.5^0(101), 47.9^0(101) and 54.2^0(101), respectively. The characteristic peak of MWNTs could be hardly identified from the patterns of TiO_2 composites as the correspondence of MWNTs reflection overlapped the anatase reflection. However, all the TiO_2 composites presented the symmetric peaks of anatase reflection in their diffraction patterns [12,41,53]. In addition, the TiO_2 crystalline sizes on the intense peak of (101) reflection were in the range of 9-13 nanometers.

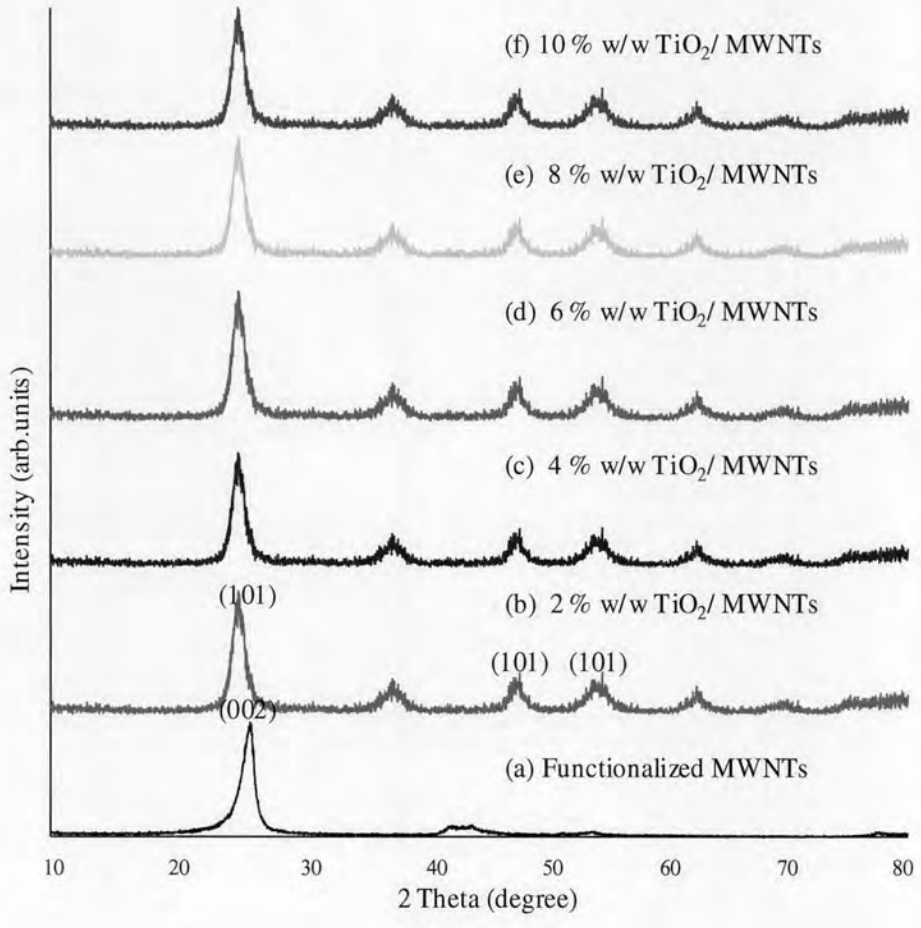

Figure 4.7 XRD patterns of (a) functionalized MWNTs and (b, c, d, e and f) 2, 4, 6, 8 and 10 % w/w of TiO_2/MWNTs composites.

4.2.2 Electrochemical Measurements of TiO_2/MWNTs Composites

In Figure 4.8, the functionalized MWNTs presented voltammetric curve like rectangular shape. The presence of symmetric curve of MWNTs electrode resulted from double layer capacitance behavior which was attributed to non faradaic process on MWNTs. Whereas, the CV curves of the nanocrystalline composite thin films exhibited the broad asymmetric redox peaks in both of anodic and cathodic scan because of the combination of double layer capacitance and pseudo capacitance contributing to total capacitance which resulted in the area of voltammetric curves was increased with metal oxide functionalizations [42-54]. Therefore, the impregnation of metal oxides on modified MWNTs surface significantly increased the electrochemical properties of the nanocomposites. In this result, it was found that the area of curves increased with the quantity of the loaded TiO_2 particles and the impregnation with 10 % w/w of TiO_2 provided the highest voltammetric area among those of other ratio of the TiO_2 composites.

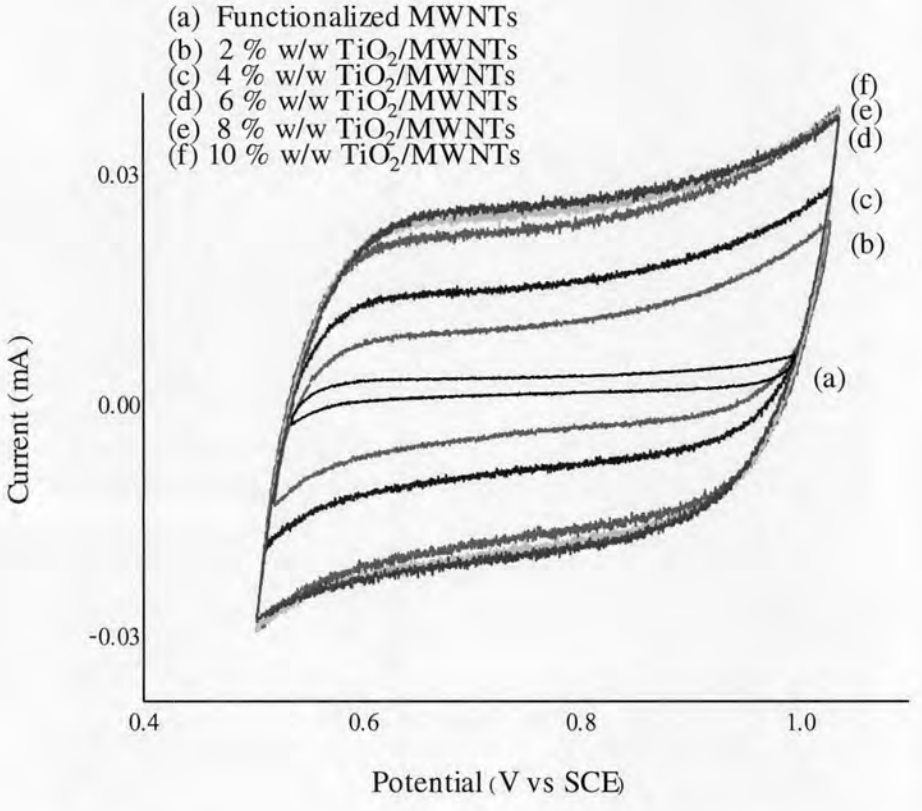

Figure 4.8 Cyclic voltammogram of (a) functionalized MWNTs and (b, c, d, e and f) MWNTs composites with 2, 4, 6, 8 and 10 % w/w of TiO_2.

The electrochemical impedance technique had been employed in order to study the difference in the electrochemical behavior between the functionalized MWNTs and the nanocrystalline composites. A semicircular loop at high frequency region could be assigned to the surface resistance and capacitance. The semicircle observed was attributed to charge transfer at the interface between the surface and active mass, couple with the double layer capacitance. In addition, a straight line at low frequency region reflected the solid state diffusion of ions into the active mass [7]. Typical complex plane plots for comparison of the modified CNTs and the TiO_2 composites are presented in Figure 4.9. The decreasing semicircle sizes were observed in the EIS plot of the functionalized MWNTs and the ratio of 2, 4, 6, 8 and 10 % w/w of TiO_2 in the composite electrodes, respectively.

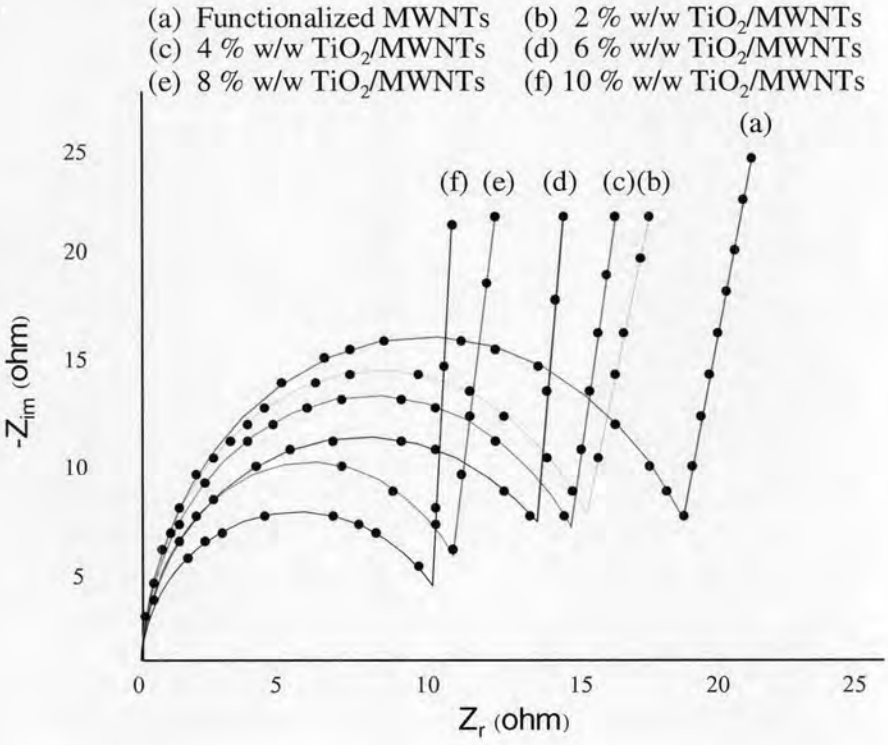

Figure 4.9 Complex-plane impedance spectra of (a) functionalized MWNTs and (b, c, d, e and f) MWNTs composites with 2, 4, 6, 8 and 10 % w/w of TiO_2.

Galvanostatic charge-discharge behaviors of functionalized MWNTs and TiO_2 composites are showed in Figure 4.10. There was an obvious difference in the slopes of the curves when compared to the functionalized MWNTs. In the case of TiO_2 composites, the slope of symmetrical charge-discharge curves was decreased with the increase in deposited metal oxide particles. The various amount of the

coated TiO_2 is presented in Figure 4.11. It was found that the composite of 10 % w/w of TiO_2 provided the longest-term cycle stability and the highest specific capacitance of 177.32 F/g.

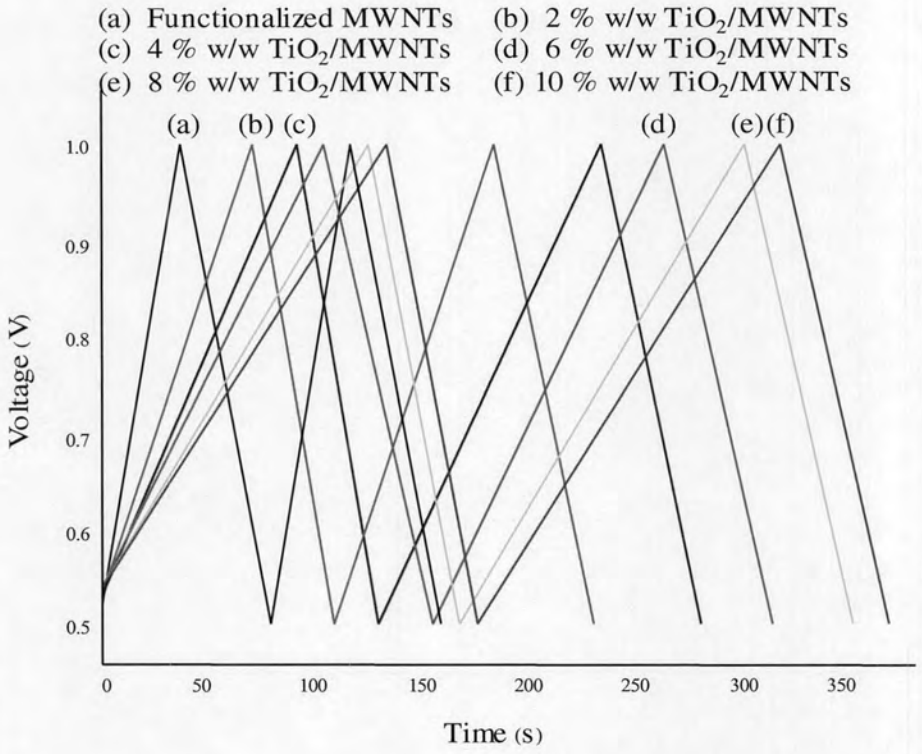

Figure 4.10 Galvanostatic charge-discharge of (a) functionalized MWNTs and (b, c, d, e and f) MWNTs composites with 2, 4, 6, 8 and 10 % w/w of TiO_2.

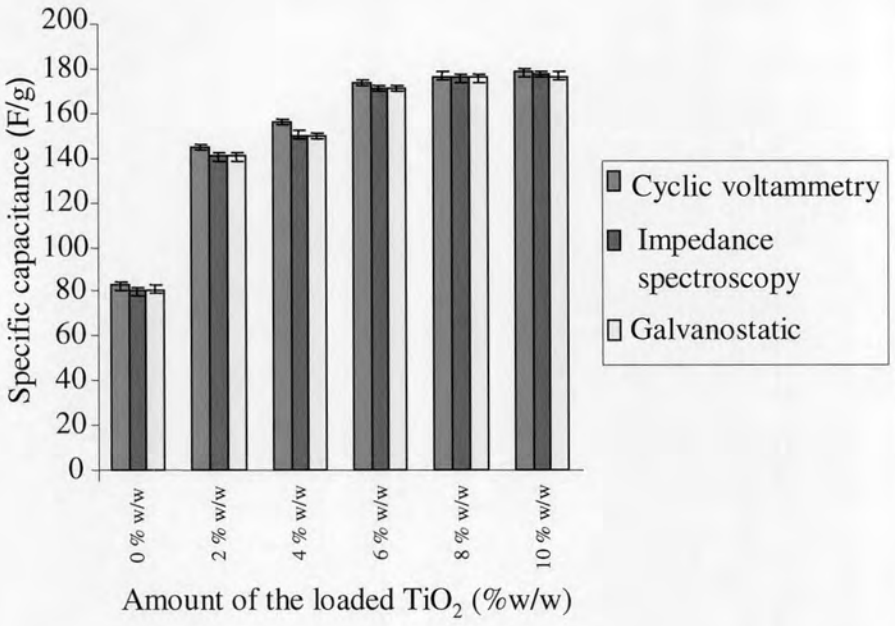

Figure 4.11 The effect of the amount of the loaded TiO_2 in MWNTs composites on specific capacitance (F/g).

4.3 Characterization of FeO/MWNTs Composites

4.3.1 Structural Characterization of FeO/MWNTs Composites

As showed in Figure 4.12 (b-f), the XRD patterns of FeO nanocrystalline composites showed a typical peak of the (002) refraction at 2θ of MWNTs at 26.3^0 and the diffraction peaks of FeO on the MWNTs surface at 31.1^0(311) and 34.7^0(311), respectively. From the Scherrer equation on the intense peak of (311) reflection, FeO crystalline sizes were determined to be in the range of 19-29 nanometers.

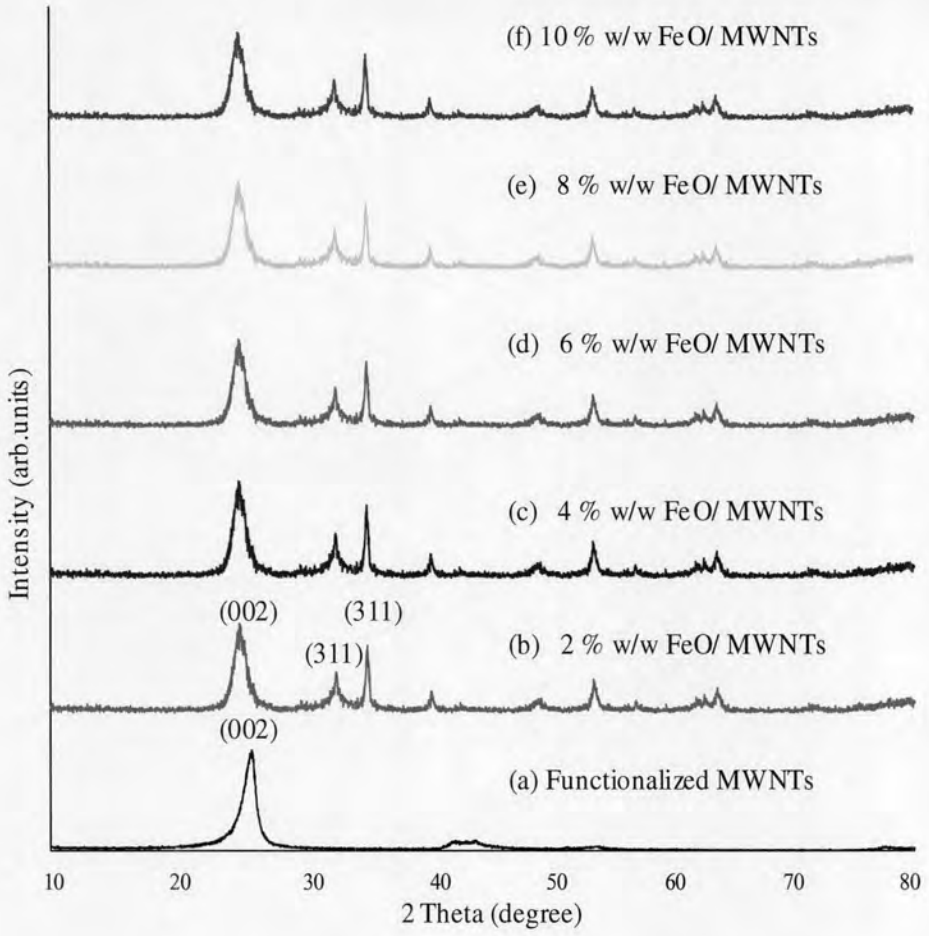

Figure 4.12 XRD patterns of (a) functionalized MWNTs and (b, c, d, e and f) 2, 4, 6, 8 and 10 % w/w of FeO/MWNTs composites.

4.3.2 Electrochemical Measurements of FeO/MWNTs Composites

The amount of FeO deposited on the modified MWNTs was 2, 4, 6, 8 and 10 % w/w, respectively. Figure 4.13 shows the increasing of capacitive current for the FeO composites. Whereas, the diameter of EIS loops in Figure 4.14 decreased slightly as well as the decrease in symmetrical charge-discharge slopes in Figure 4.15 resulted from the amount of the deposited nanocrystalline metal oxide. These results indicated that the electrochemical characteristic responded with respect to the mass of FeO in the samples which resulted in the higher pseudo-capacitive behavior of metal oxide as illustrated in Figure 4.16. Moreover, the average specific capacitance of the composite contained 10 % w/w of FeO was 105.27 F/g.

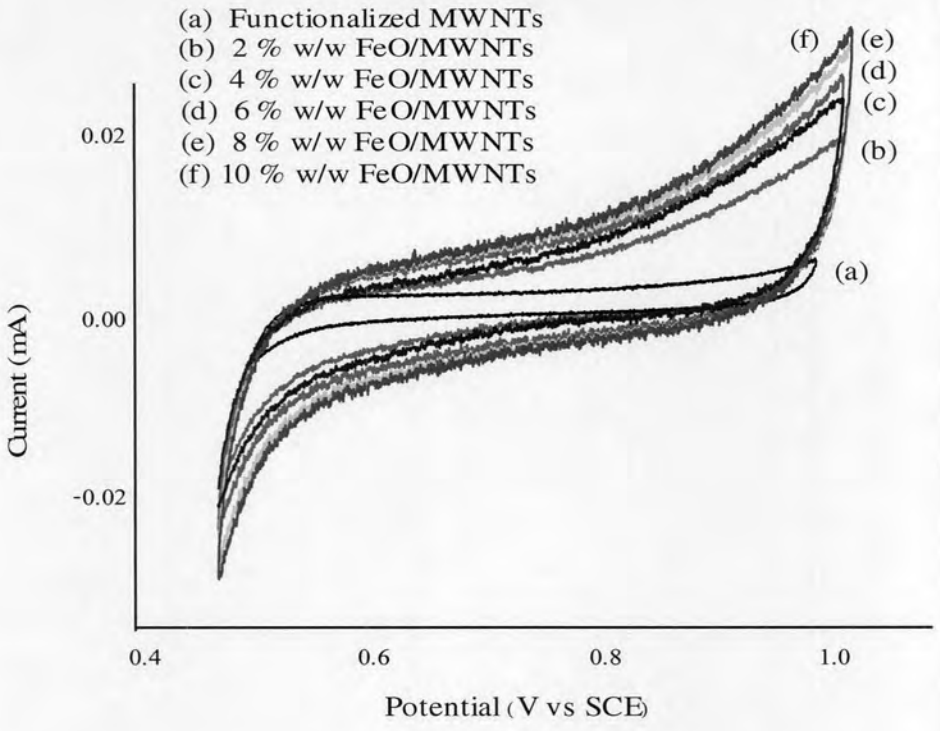

Figure 4.13 Cyclic voltammogram of (a) functionalized MWNTs and (b, c, d, e and f) MWNTs composites with 2, 4, 6, 8 and 10 % w/w of FeO.

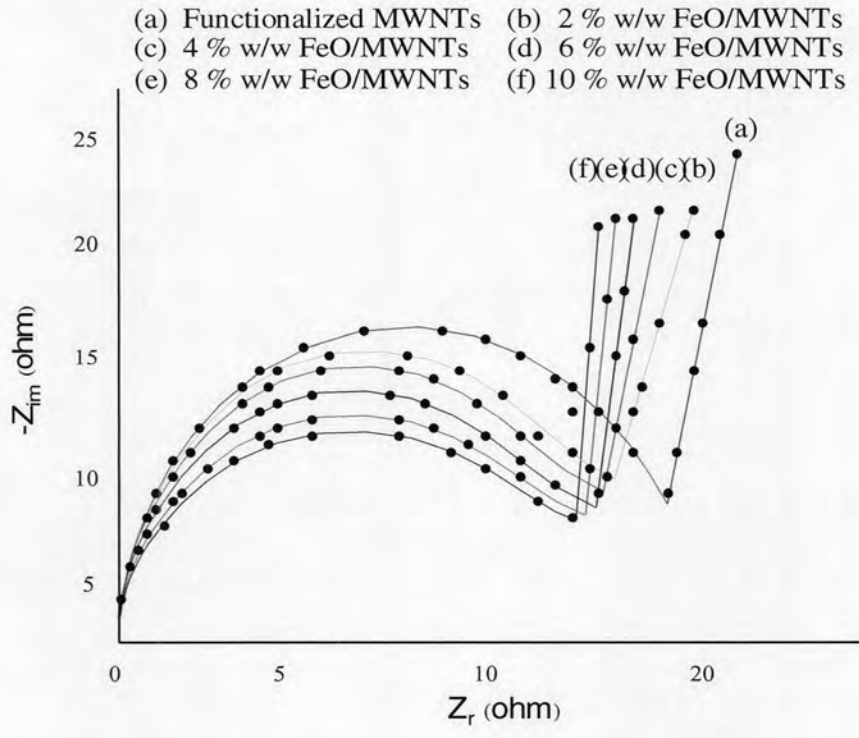

Figure 4.14 Complex-plane impedance spectra of (a) functionalized MWNTs and (b, c, d, e and f) MWNTs composites with 2, 4, 6, 8 and 10 % w/w of FeO.

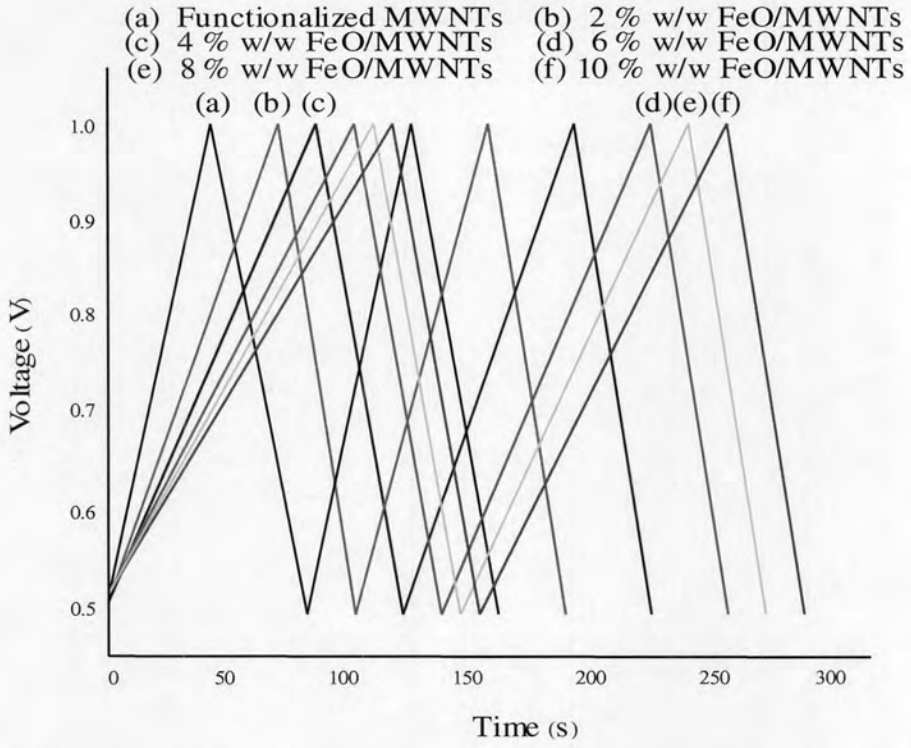

Figure 4.15 Galvanostatic charge-discharge of (a) functionalized MWNTs and (b, c, d, e and f) MWNTs composites with 2, 4, 6, 8 and 10 % w/w of FeO.

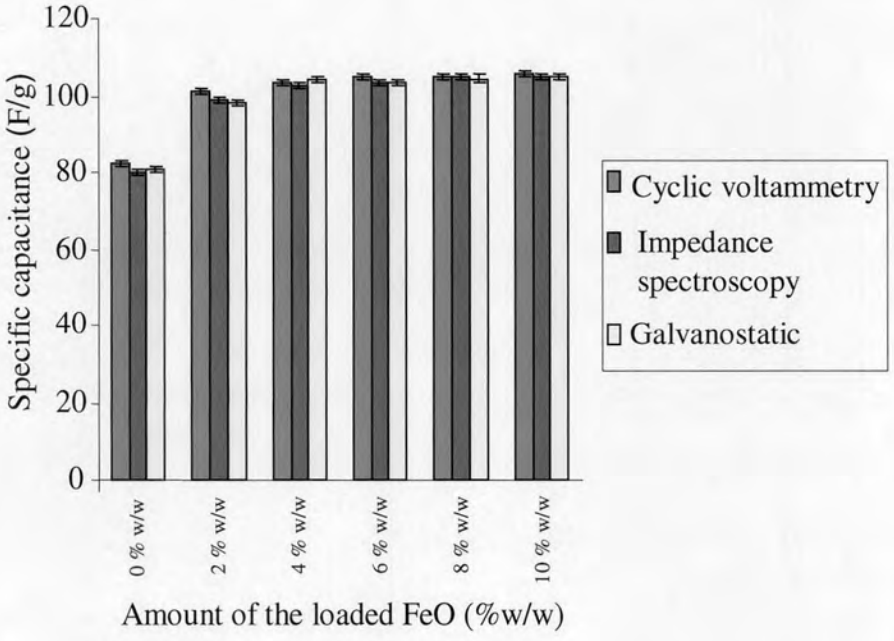

Figure 4.16 The effect of the amount of the loaded FeO in MWNTs composites on specific capacitance (F/g).

4.4. Characterization of NiO/MWNTs Composites

4.4.1 Structural Characterization of NiO/MWNTs Composites

Figure 4.17 (b-f) illustrate the XRD patterns for different ratio of NiO in MWNTs nanocomposites. Characteristic peak located at 26.3^0 corresponded to the (002) plane of MWNTs and NiO could be indexed at 35.2^0(111), 41.3^0(220) and 62.6^0(220), respectively [20,21]. Moreover, the NiO crystalline sizes on the MWNTs surface were found to be in the range of 9-10 nanometers.

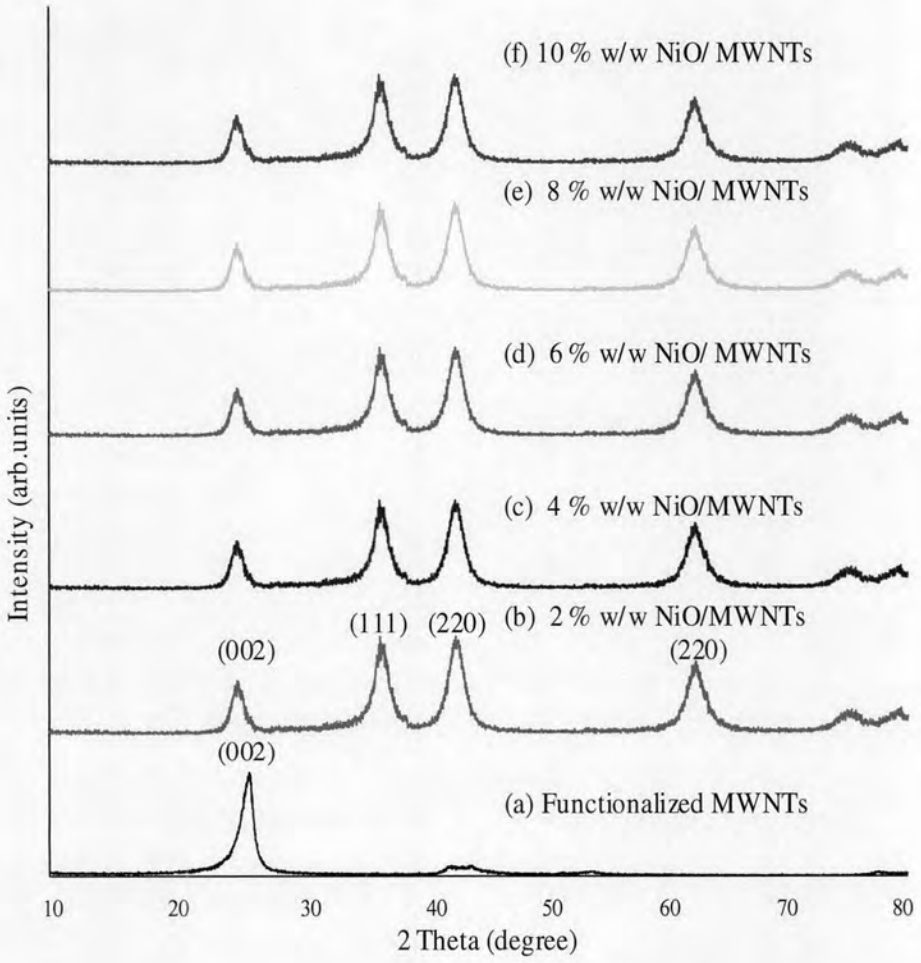

Figure 4.17 XRD patterns of (a) functionalized MWNTs and (b, c, d, e and f) 2, 4, 6, 8 and 10 % w/w of NiO/MWNTs composites.

4.4.2 Electrochemical Measurements of NiO/MWNTs Composites

The comparison of cyclic voltammograms between the pure MWNTs and the NiO-loaded MWNTs is presented in Figure 4.18. It could be seen that the voltammetric curves for the NiO composites were increased when a loading of nickel (II) nitrate with the functionalized MWNTs also increased while Figure 4.19 illustrates the decrease in the diameter of EIS loops as well as the slope of symmetrical charge-discharge curves decreased in Figure 4.20. Thus, NiO quantity in the composites has the influence on the specific capacitance of the capacitor electrodes. In this study, the specific capacitance of the modified MWNTs was enhanced from 81.21 to 170.78 F/g for the composite with 10 % w/w of deposited NiO as presented in Figure 4.21.

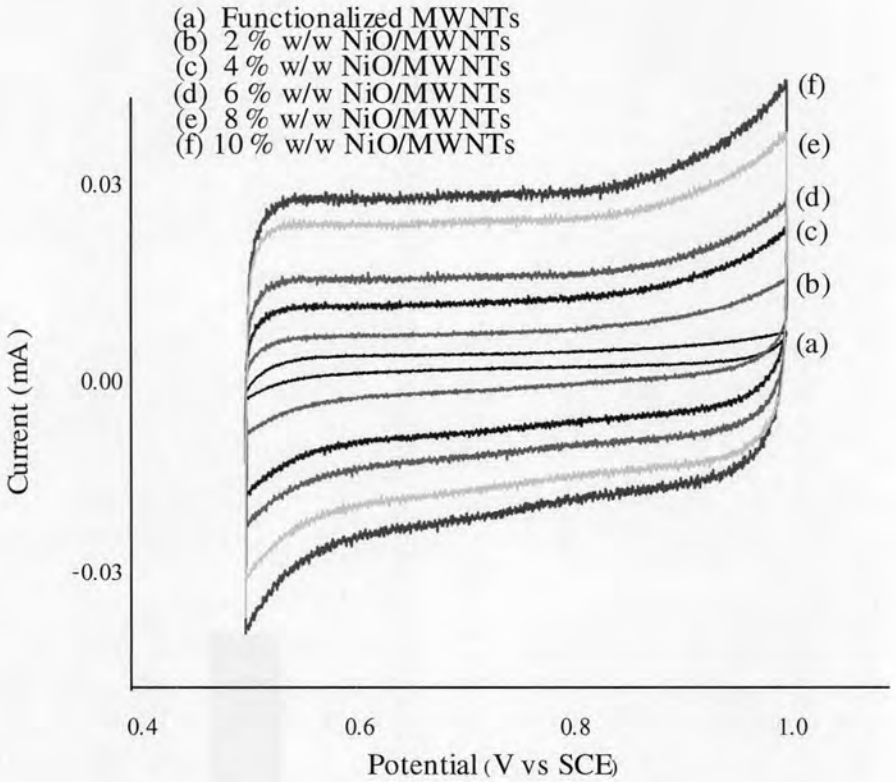

Figure 4.18 Cyclic voltammogram of (a) functionalized MWNTs and (b, c, d, e and f) MWNTs composites with 2, 4, 6, 8 and 10 % w/w of NiO.

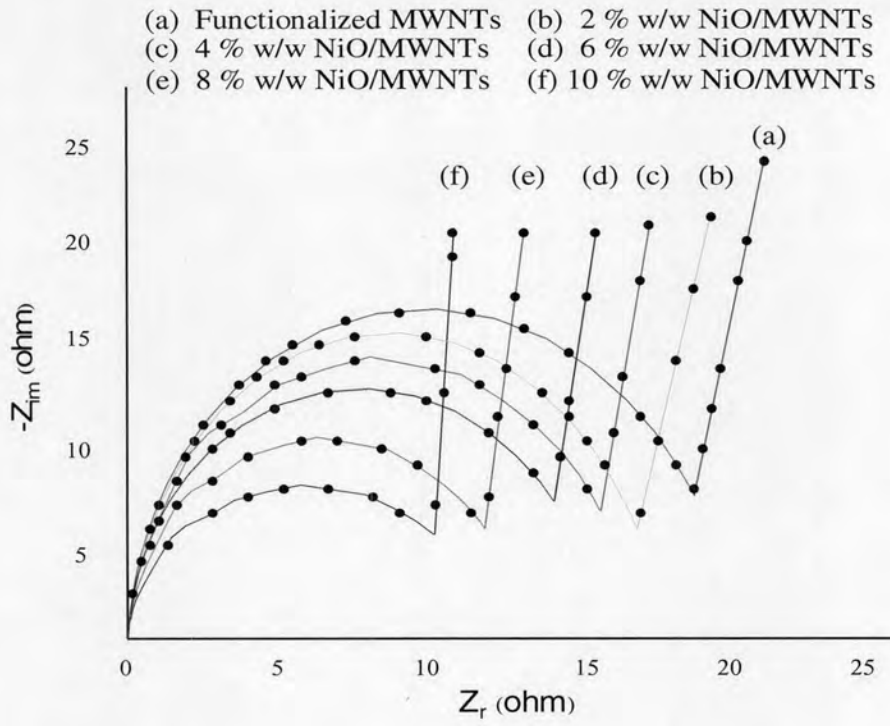

Figure 4.19 Complex-plane impedance spectra of (a) functionalized MWNTs and (b, c, d, e and f) MWNTs composites with 2, 4, 6, 8 and 10 % w/w of NiO.

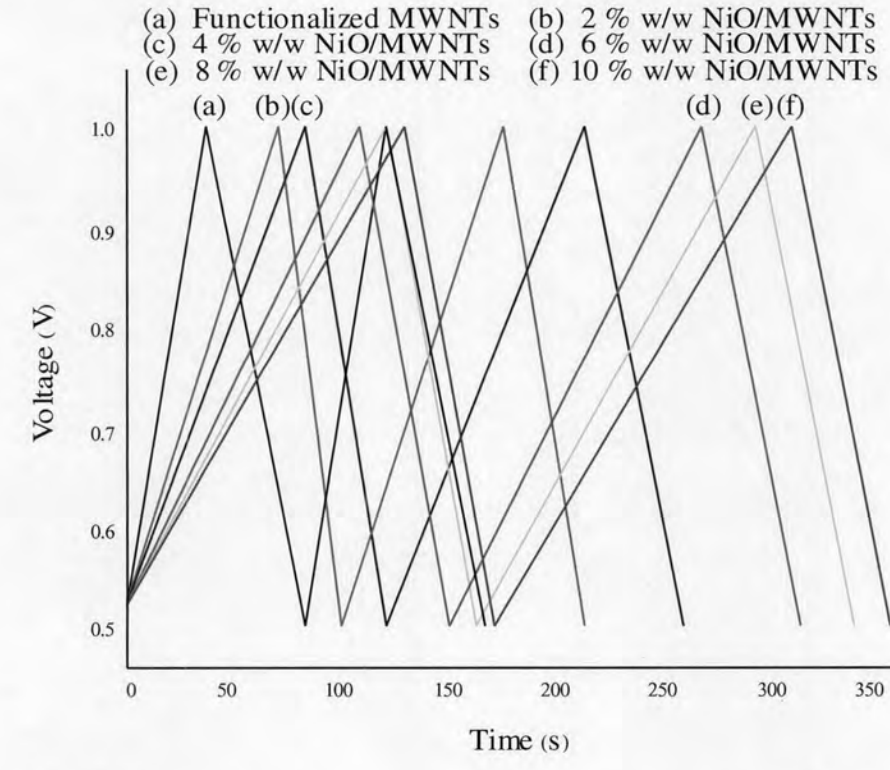

Figure 4.20 Galvanostatic charge-discharge of (a) functionalized MWNTs and (b, c, d, e and f) MWNTs composites with 2, 4, 6, 8 and 10 % w/w of NiO.

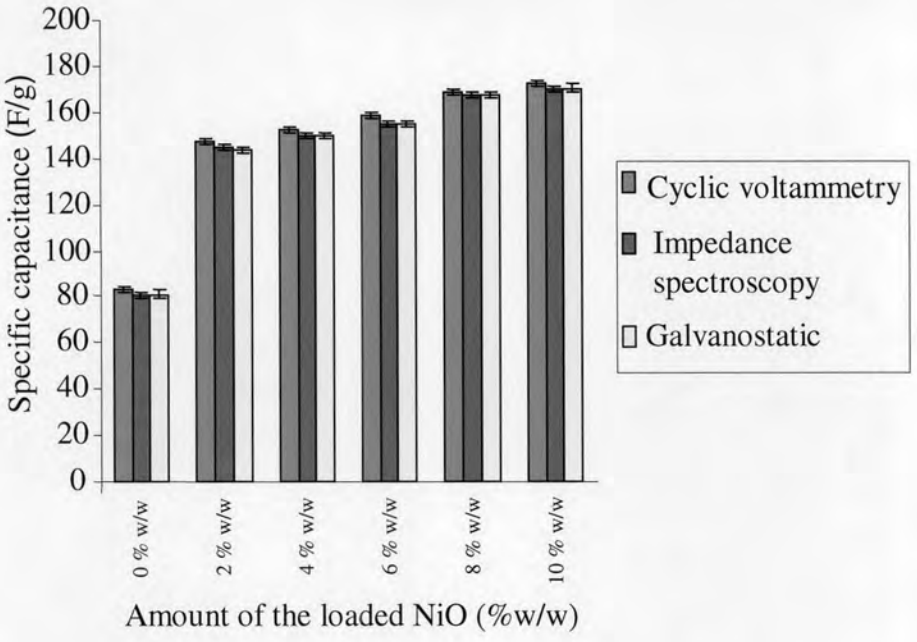

Figure 4.21 The effect of the amount of the loaded NiO in MWNTs composites on specific capacitance (F/g).

4.5 Characterization of FeO-TiO_2/MWNTs Composites

4.5.1 Structural Characterization of FeO-TiO_2/MWNTs Composites

As showed in Figure 4.22 (b-e), the XRD patterns of FeO-TiO_2/MWNTs nanocomposites showed a typical peak of the (101) refraction at 2θ of TiO_2 in anatase phase at 25.5^0, which overlap the (002) reflection of MWNTs at 26.3^0, 47.9^0(101) and 54.2^0(101), respectively. The diffraction peaks of FeO in TiO_2/MWNTs composites at 31.1^0(311) and 34.7^0(311), respectively. More interestingly, from the Scherrer equation using the intense peak of (101) and (311) reflection, the crystalline sizes of TiO_2 and FeO were determined to be 10 and 32 nanometers, respectively.

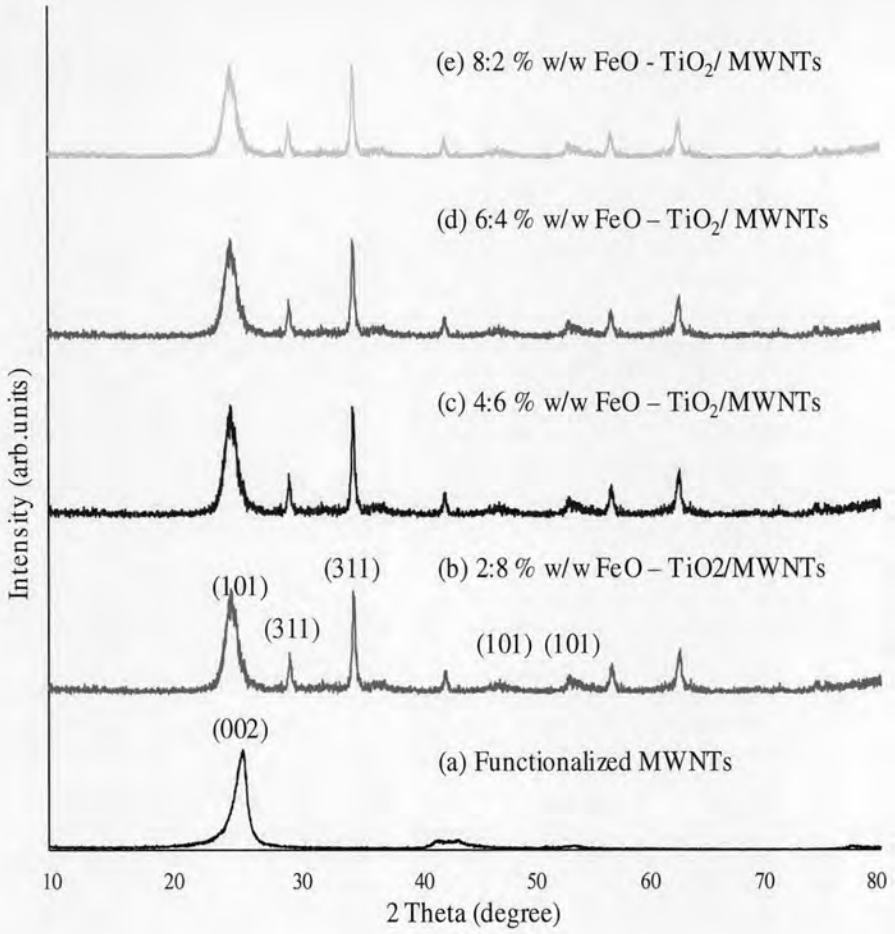

Figure 4.22 XRD patterns of (a) functionalized MWNTs and (b, c, d and e) MWNTs composites with 2:8, 4:6, 6:4 and 8:2 % w/w of FeO:TiO_2.

4.5.2 Electrochemical Measurements of FeO-TiO_2/MWNTs Composites

In Figure 4.23, cyclic votammogram of FeO-TiO_2/MWNTs composites presented the decreasing of the area of voltammetric curves, caused by the amount of nanocrystalline FeO in the TiO_2 composites, while the diameter of semicular loops in Figure 4.24 increased as well as the increase in the slope of the symmetrical charge-discharge curves in Figure 4.25 which exhibited the lower cycle stability. Importantly, the comparison of electrochemical properties for the FeO-TiO_2 composites with those of the TiO_2/MWNTs composites in figure 4.8, 4.9 and 4.10 revealed the average capacitances for FeO-TiO_2 composites were lower than those of TiO_2 composites. These results implied that the electrochemical property of FeO was insulator, it could not provide the effective faradaic reaction of pseudo-capacitive behavior as showed in Figure 4.26. Nevertheless, the maximum average capacitance

was 123.01 F/g for the composite with 2:8 % w/w of FeO:TiO_2 and the average specific capacitance of another FeO-TiO_2 composites was the same.

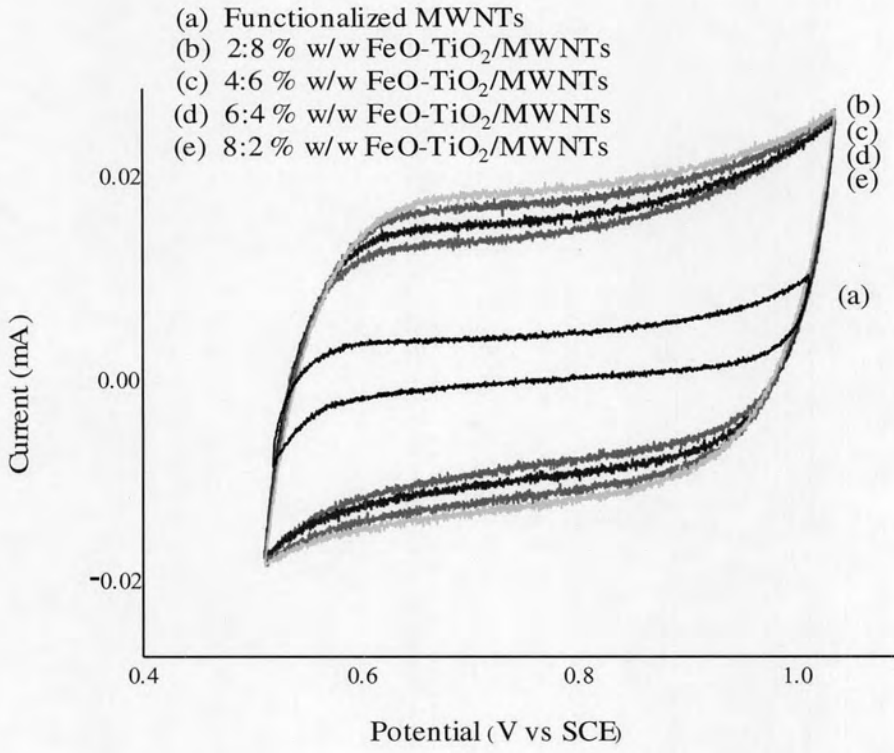

Figure 4.23 Cyclic voltammogram of (a) functionalized MWNTs and (b, c, d and e) MWNTs composites with 2:8, 4:6, 6:4 and 8:2 % w/w of FeO:TiO_2.

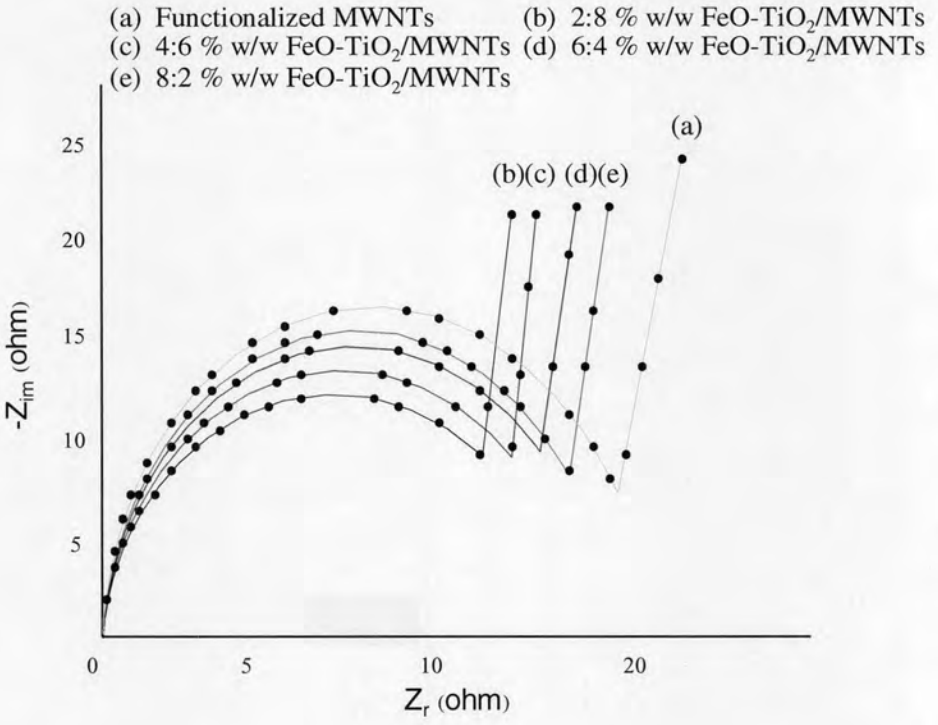

Figure 4.24 Complex-plane impedance spectra of (a) functionalized MWNTs and (b, c, d and e) MWNTs composites with 2:8, 4:6, 6:4 and 8:2 % w/w of $FeO:TiO_2$.

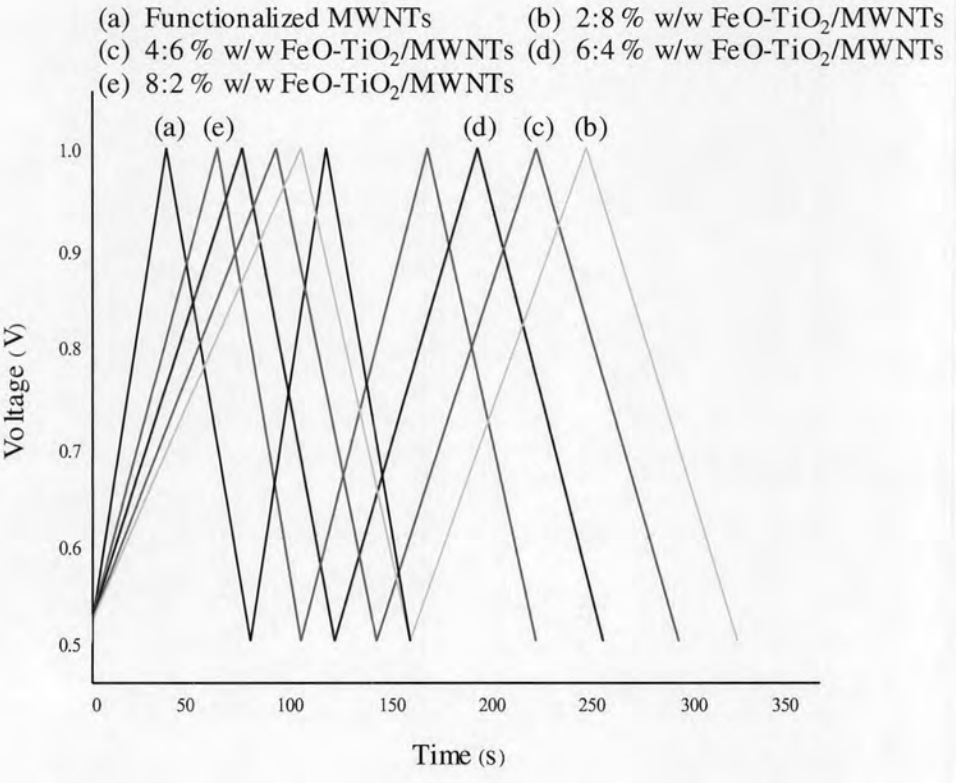

Figure 4.25 Galvanostatic charge-discharge of (a) functionalized MWNTs and (b, c, d and e) MWNTs composites with 2:8, 4:6, 6:4 and 8:2 % w/w of $FeO:TiO_2$.

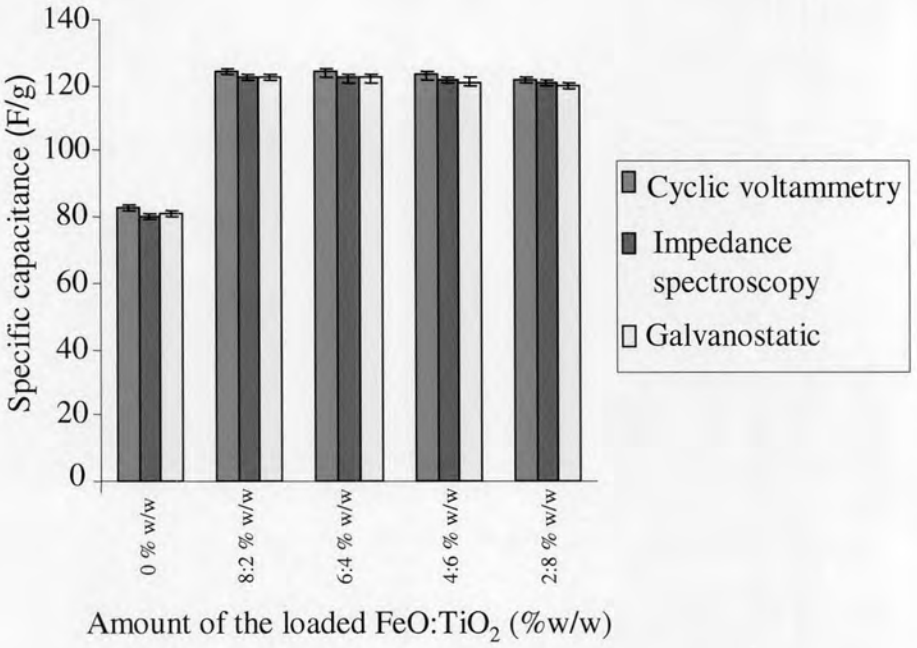

Figure 4.26 The effect of the amount of $FeO:TiO_2$ in MWNTs composites on specific capacitance (F/g).

4.6 Characterization of NiO-TiO_2/MWNTs Composites

4.6.1 Structural Characterization of NiO-TiO_2/MWNTs Composites

The XRD patterns in Figure 4.27 (b-f) illustrate the ratio of $NiO:TiO_2$ on MWNTs surface. Characteristic peaks located at 25.5^0, 47.9^0 and 54.2^0 correspond to the (101) plane of TiO_2 in anatase phase. In addition, NiO could be indexed at 35.2^0(111), 41.3^0(220) and 62.6^0(220), respectively. From the Scherrer equation using the intense peak of (101) and (111) reflection, TiO_2 crystalline size on the MWNTs surface was found to be 10 nanometers, while NiO particle sizes were in the range of 9-10 nanometers, respectively.

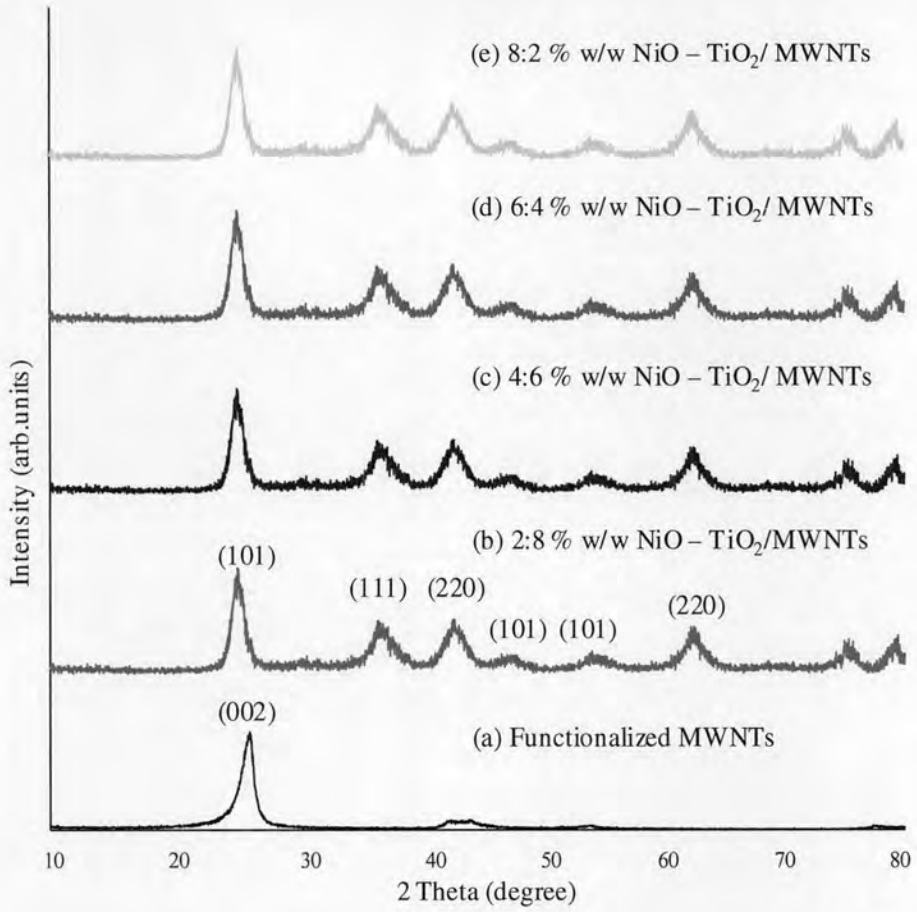

Figure 4.27 XRD patterns of (a) functionalized MWNTs and (b, c, d and e) MWNTs composites with 2:8, 4:6, 6:4 and 8:2 % w/w of NiO:TiO_2.

4.6.2 Electrochemical Measurements of NiO-TiO_2/MWNTs Composites

Cyclic votammograms for modified MWNTs and NiO-TiO_2/MWNTs composites are present in Figure 4.28. It was found that the area of voltammetric curves was increased closely with the amount of NiO particles on the TiO_2 composite surface whereas the EIS plots in Figure 4.29 show the decrease in the semicircles. The slope of the symmetrical charge-discharge curves in Figure 4.30 also decreased which implied the longer cycle life of composites. In addition, the average specific capacitance of each sample was not different. However, the maximum average capacitance was 180.40 F/g for the composite with 4:6 % w/w of NiO:TiO_2 as illustrated in Figure 4.31. More interestingly, the comparison of average capacitances for the NiO-TiO_2 composites with that for the TiO_2/MWNTs composites in Figure 4.8, 4.9 and 4.10 revealed the average capacitances for NiO-TiO_2 composites were higher

than the TiO_2 composites. This result implied that the electrochemical property of NiO was electroactivator, performing the pseudo-capability behavior.

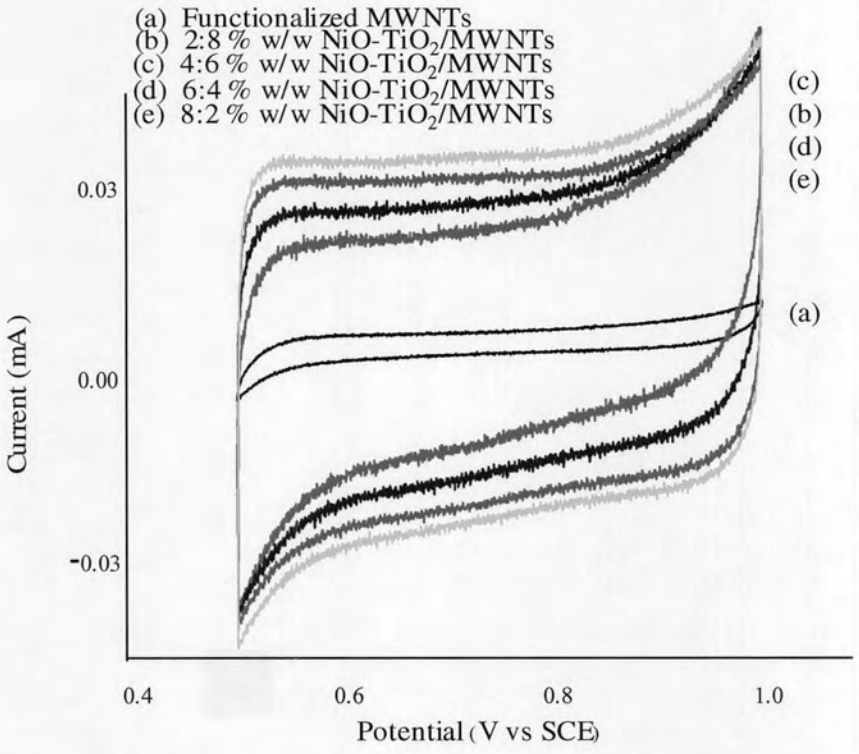

Figure 4.28 Cyclic voltammogram of (a) functionalized MWNTs and (b, c, d and e) MWNTs composites with 2:8, 4:6, 6:4 and 8:2 % w/w of $NiO:TiO_2$.

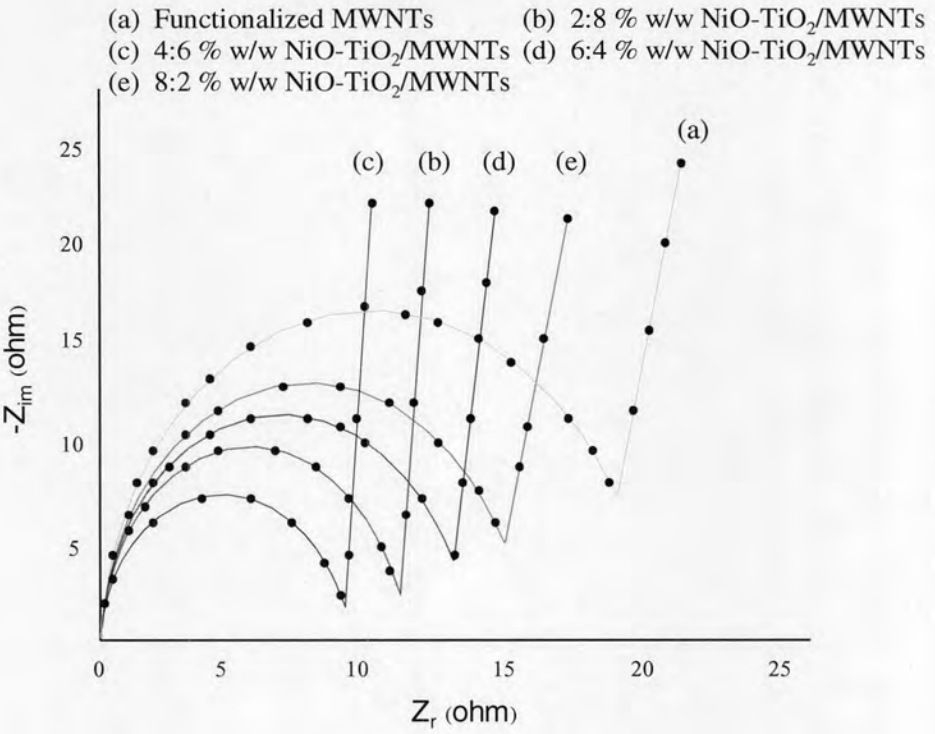

Figure 4.29 Complex-plane impedance spectra of (a) functionalized MWNTs and (b, c, d and e) MWNTs composites with 2:8, 4:6, 6:4 and 8:2 % w/w of $NiO:TiO_2$.

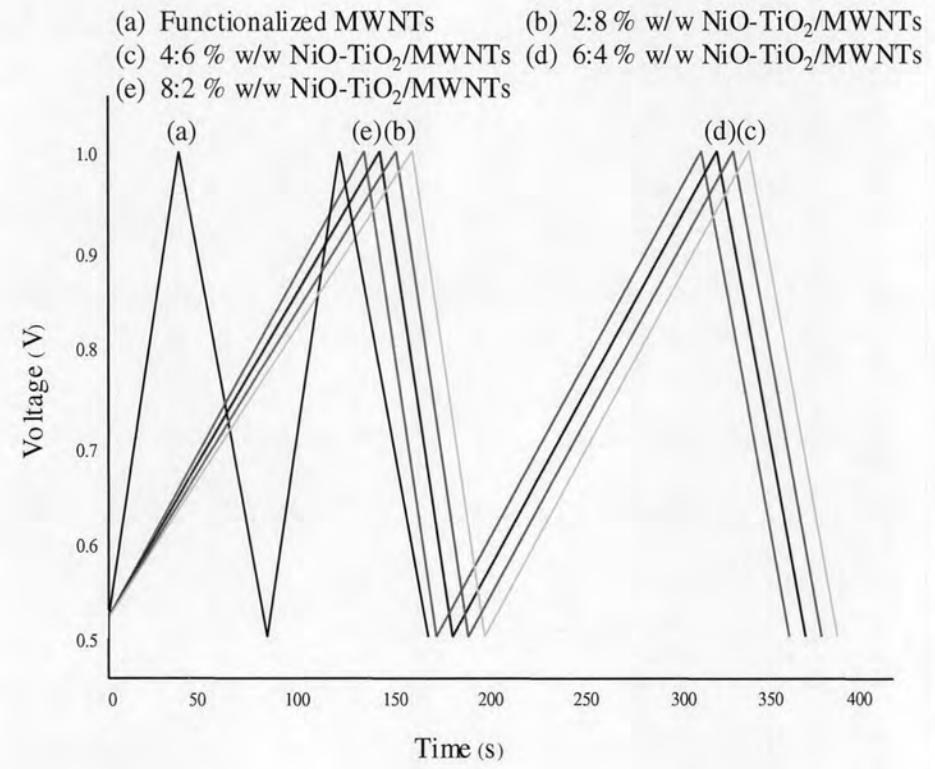

Figure 4.30 Galvanostatic charge-discharge of (a) functionalized MWNTs and (b, c, d and e) MWNTs composites with 2:8, 4:6, 6:4 and 8:2 % w/w of $NiO:TiO_2$.

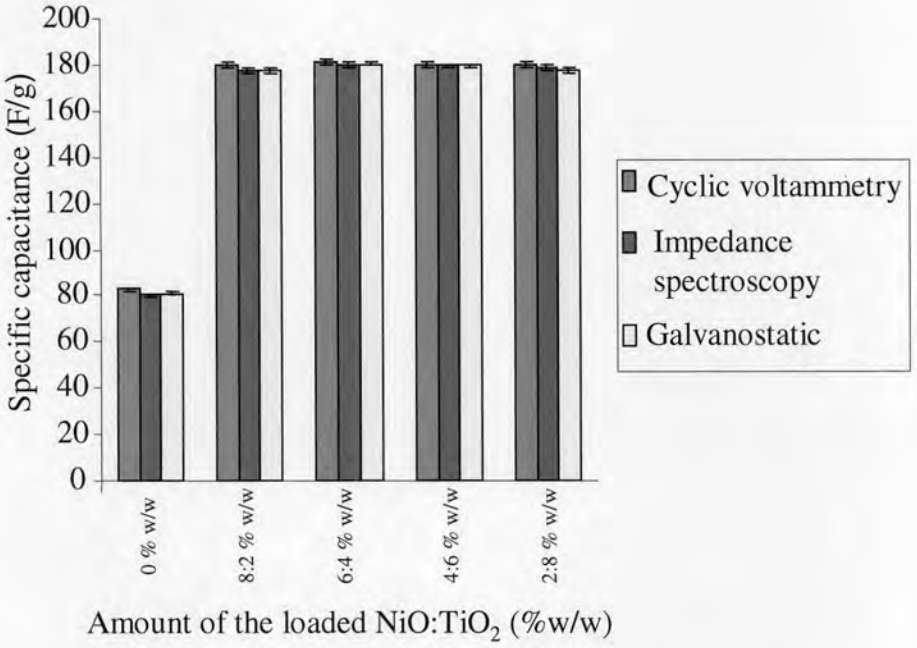

Figure 4.31 The effect of the amount of $NiO:TiO_2$ in MWNTs composites on specific capacitance (F/g).

4.7 Comparison of MWNTs and Titanium - Based Oxide Composites

4.7.1 Comparison of Structural Characterization

XRD analysis, which is the most useful technique for identification of crystalline structure, was employed to investigate the prepared samples. As showed in Figure 4.32 (a), the XRD pattern of as received MWNTs using nickel as catalyst during preparation process. Characteristic peak, which appeared at 2θ values of 26.3^0(002) for the MWNTs, was indicated to reflect hexagonal graphite. Other small peaks corresponding to the catalytic impurities were also observed. The XRD pattern of the functionalized MWNTs in Figure 4.32 (b) indicated that the metallic impurities of the MWNTs were removed by acid treatment. Figure 4.32 (c) illustrates the XRD pattern of TiO_2 in anatase phase of TiO_2 composites at 25.5°(101), 47.9°(101) and 54.2°(101). Characteristic peak of MWNTs was found hardly identified from the pattern of the TiO_2 composites. Although the reflection of MWNTs overlapped the anatase reflection, all the TiO_2 composites presented symmetric peak of anatase reflection in their diffraction patterns. The broader diffraction peaks of FeO-attached on the MWNTs surface in Figure 4.26 (d) at 31.1^0(311) and 34.7^0(311) and NiO in

the synthesized sample in Figure 4.32 (e) at 35.2^0(111), 41.3^0(200) and 62.6^0(220) revealed that NiO and FeO have been crystalline structure. Hence, the nanocrytalline composites could be well prepared by chemical reduction and these products could be finally converted to the crystallized phase by heating treatment. Besides, they could be clearly seen NiO and FeO scattered throughout the TiO_2 /MWNTs nanocomposites.

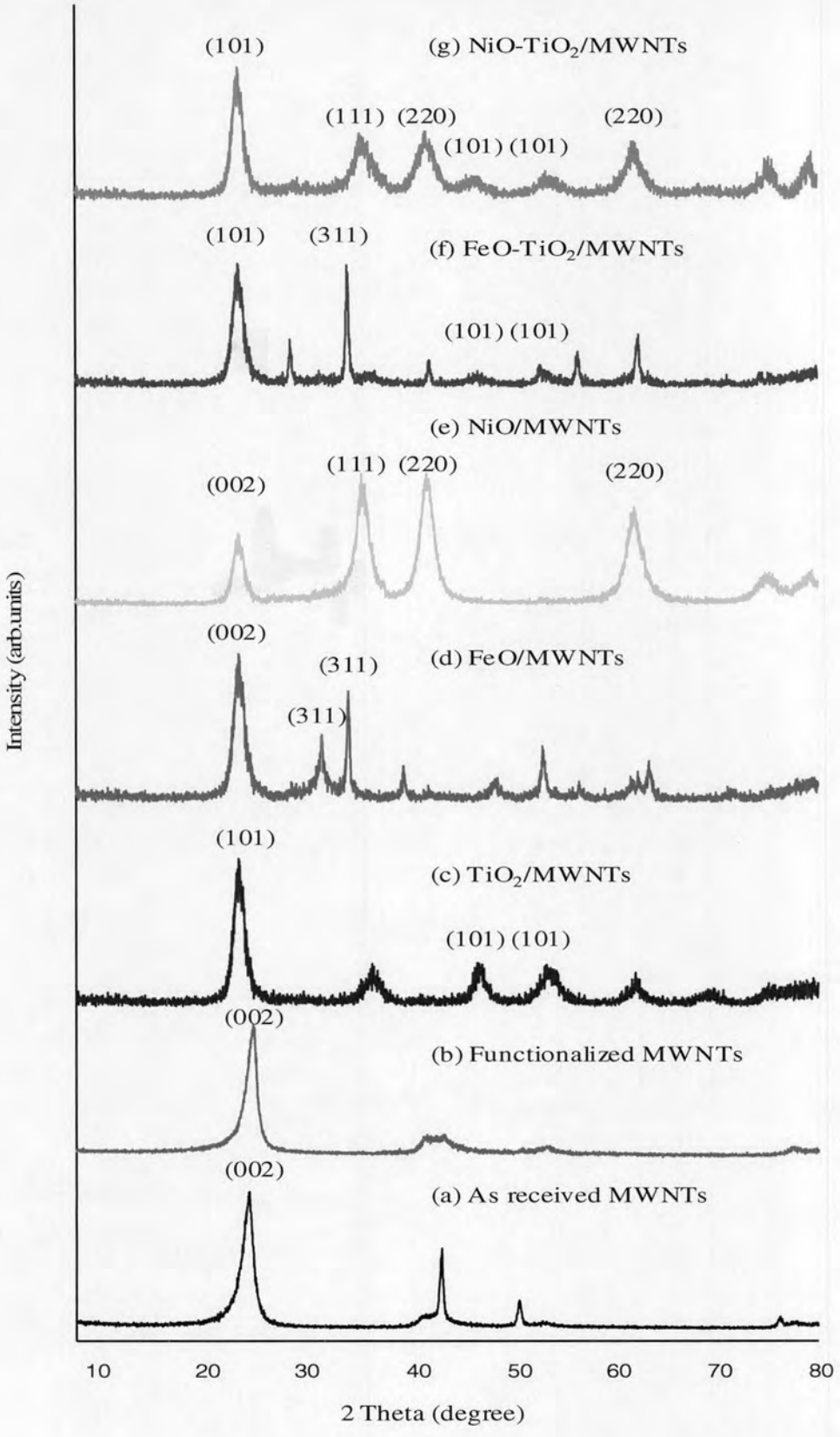

Figure 4.32 XRD patterns of (a) as received MWNTs, (b) functionalized MWNTs, (c) TiO_2/MWNTs, (d) FeO/MWNTs, (e) NiO/MWNTs, (f) FeO-TiO_2/MWNTs and (g) NiO-TiO_2/MWNTs.

4.7.2 Comparison of Morphological Characterization

The morphology of purified MWNTs and synthesized composites was investigated using SEM and TEM. The results obtained from SEM are showed in Figure 4.33 (a – d). The image of purified MWNTs indicates the good quality of the MWNTs. It is marked that the nanotubes are curved. The significant morphology difference for MWNTs and crystalline composite electrodes can be clearly observed by TEM images in Figure 4.33 (e – h). From Figure 4.33 (b – d and f – h), they reveal that crystalline nanoparticles of TiO_2, FeO and NiO attached and distributed on the surface of functionalized MWNTs in the composite samples. While purified MWNTs in Fig. 4.33 (a and e) show the distinguishable surface of the graphitized walls without any remarked coverage with other particles. Nanostructures of metal oxide are thought to be beneficial to ionic charge transport.

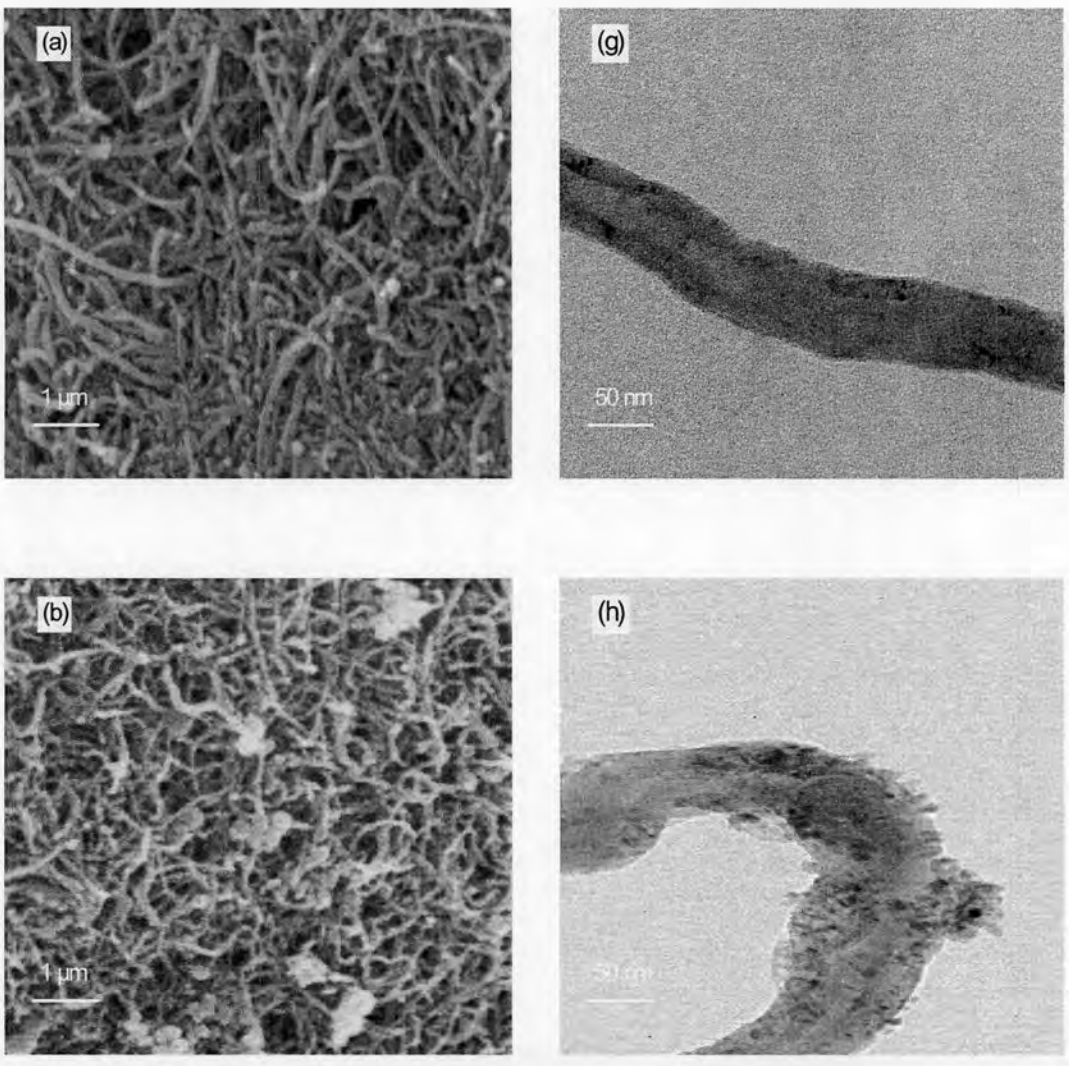

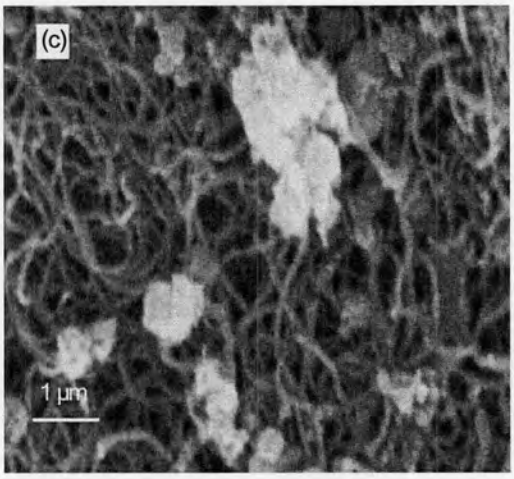
(c)
1 µm

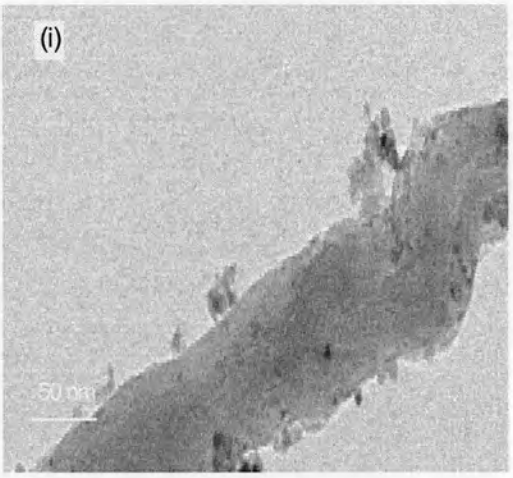
(i)
50 nm

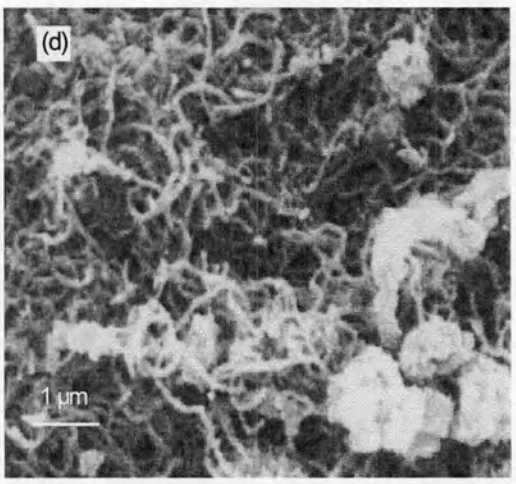
(d)
1 µm

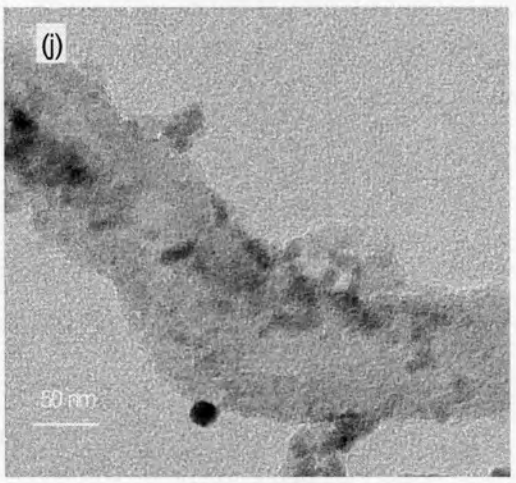
(j)
50 nm

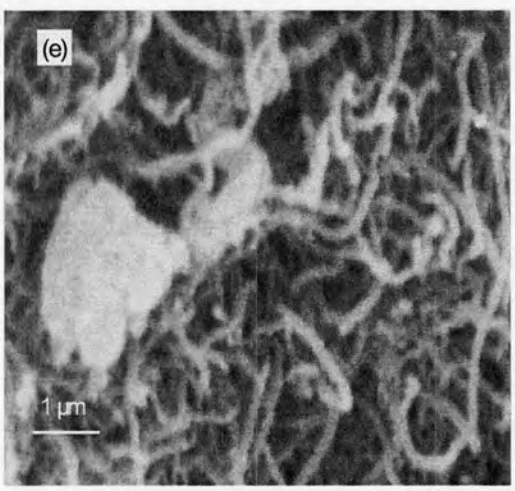
(e)
1 µm

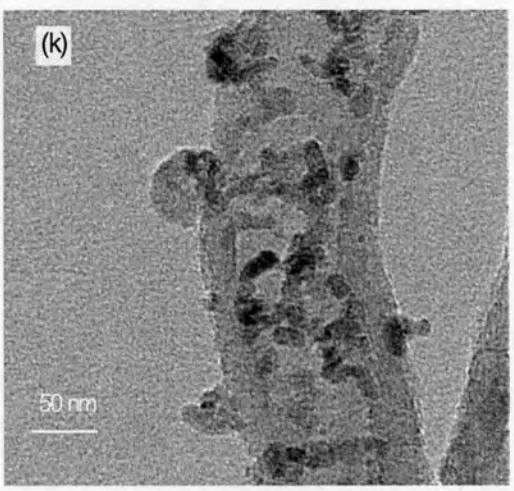
(k)
50 nm

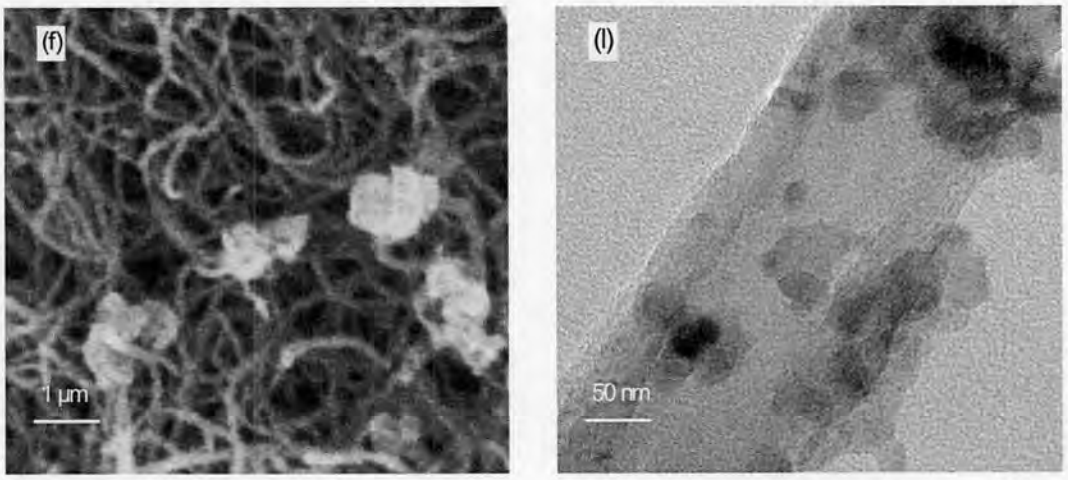

Figure 4.33 SEM images of (a) functionalized MWNTs, (b) TiO_2/MWNTs, (c) FeO/MWNTs, (d) TiO_2/MWNTs, (e) FeO-TiO_2/MWNTs and (f) NiO-TiO_2/MWNTs, TEM images of (g) the purified MWNTs, (h) TiO_2/MWNTs, (i) FeO/MWNTs, (j) NiO/MWNTs, (k) FeO -TiO_2/MWNTs and (l) NiO-TiO_2/MWNTs.

4.7.3 Electrochemical Comparison of MWNTs and Titanium - Based Oxide Composites

The electrochemical properties of the titanium-based oxide composites could be compared by three electrochemical techniques as illustrated in Figure 4.34, 4.35 and 4.36. As presented in Figure 4.37, the specific capacitance of the functionalized MWNTs, 10 % w/w of TiO_2/MWNTs, 2:8 % w/w of FeO-TiO_2/MWNTs and the 4:6 w/w % of NiO-TiO_2/MWNTs composite electrodes were 81.21, 177.32, 123.01 and 180.40 F/g, respectively. The specific capacitance of the TiO_2/MWNTs composite was higher than that of the functionalized MWNTs electrode owing to the dispersion of nanocrystalline metal oxide on modified MWNTs contributing to the combination of double layer and pseudo capacitances. Furthermore, the result of the NiO-TiO_2/MWNTs composites showed the higher capacitances and the longer cycle life, which different from the TiO_2/MWNTs nanocomposite, could be attributed to the presence of NiO-attached to the TiO_2 composite electrodes. This result implied that NiO could be the electroactivator, which had the influence on TiO_2/MWNTs capacitor performance [55]. On the contrary, FeO in TiO_2/MWNTs electrodes contributed to the decrease in capacitive

property of the composites which resulted from the electrochemical behavior of FeO was insulator [56]. This study indicated that FeO was not the suitable metal to synthesize for the composite capacitor.

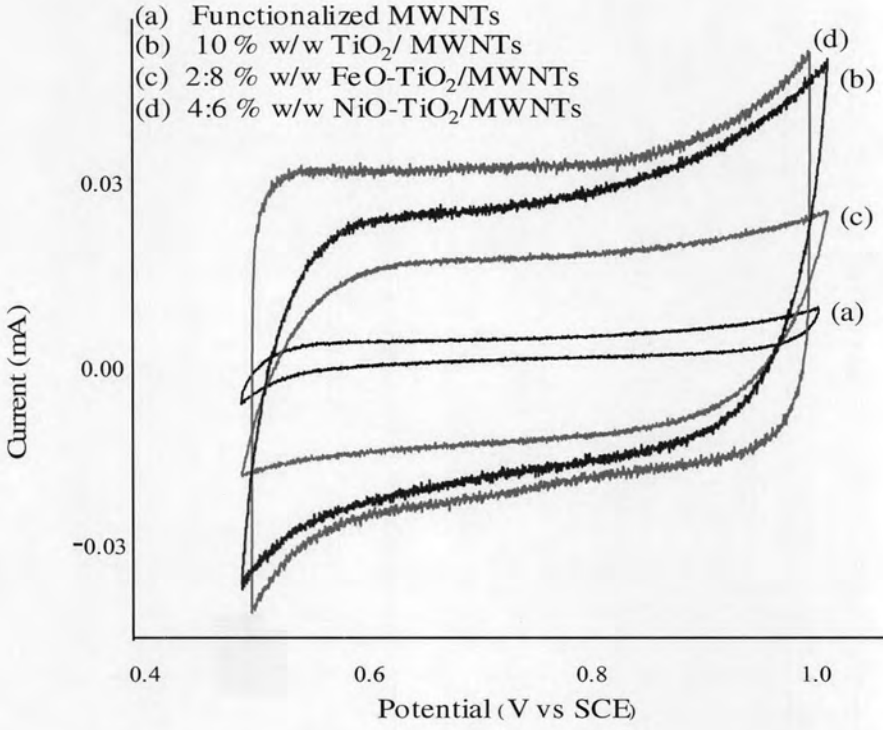

Figure 4.34 Cyclic voltammogram of (a) functionalized MWNTs, (b) 10 % w/w of TiO_2/MWNTs, (c) 2:8 % w/w of FeO-TiO_2/MWNTs and (d) 4:6 % w/w of NiO-TiO_2/MWNTs.

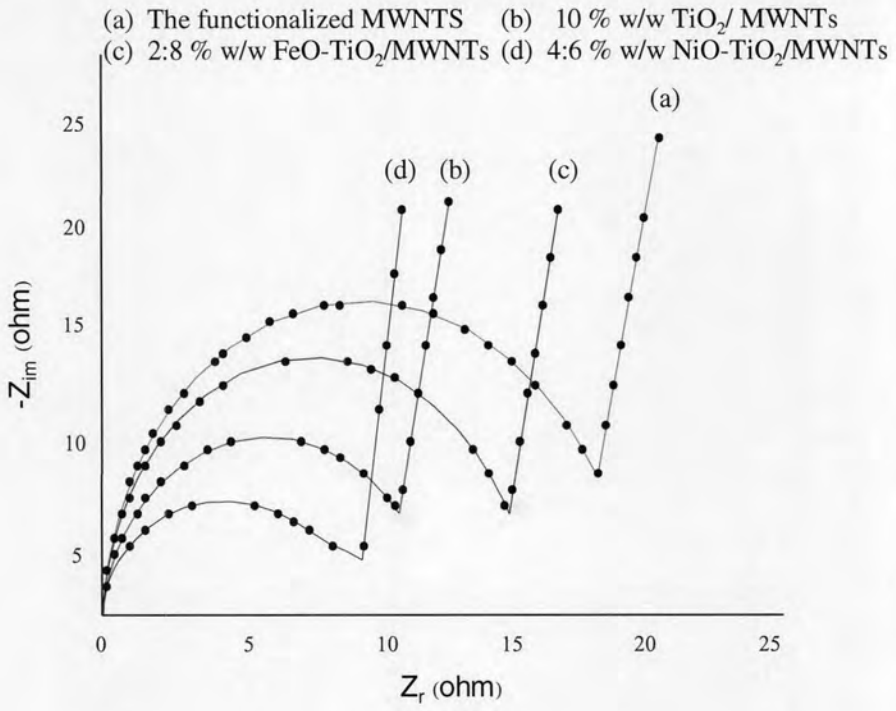

Figure 4.35 Complex-plane impedance spectra of (a) functionalized MWNTs, (b) 10 % w/w of TiO_2/MWNTs, (c) 2:8 % w/w of FeO-TiO_2/MWNTs and (d) 4:6 % w/w of NiO-TiO_2/MWNTs.

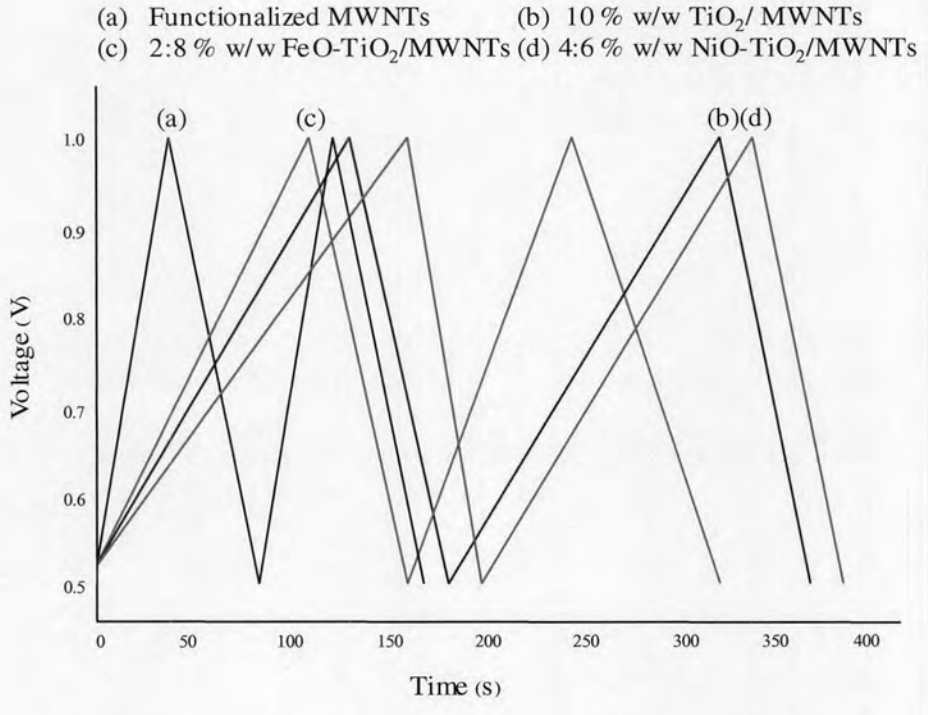

Figure 4.36 Galvanostatic charge-discharge of (a) functionalized MWNTs, (b) 10 % w/w of TiO_2/MWNTs, (c) 2:8 % w/w of FeO-TiO_2/MWNTs and (d) 4:6 % w/w of NiO-TiO_2/MWNTs.

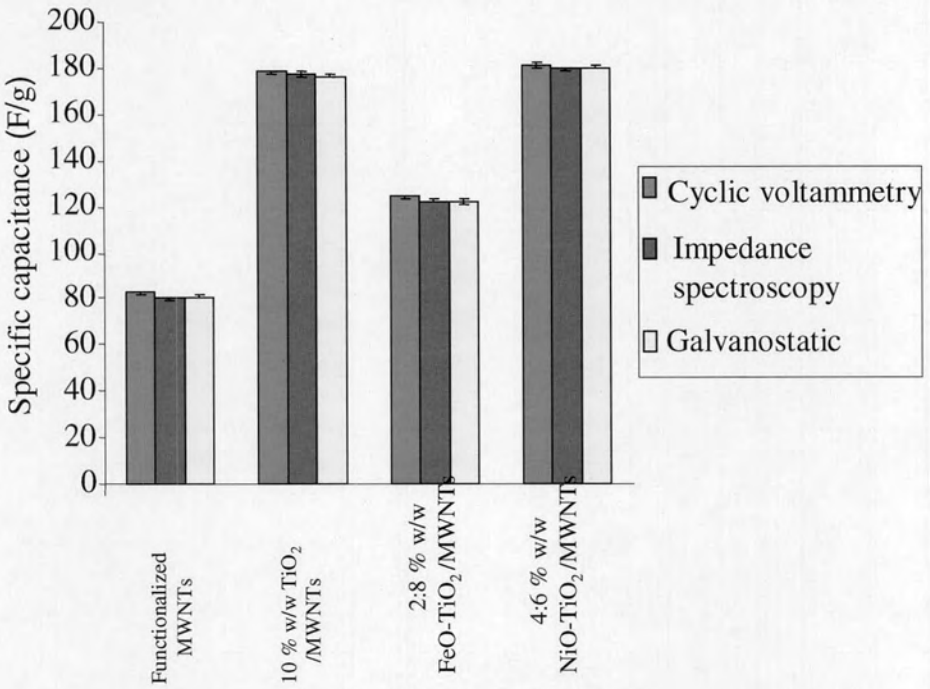

Figure 4.37 The effect of different materials on specific capacitance (F/g).